UNIVERSITY OF OKLAHOMA

GRADUATE COLLEGE

MODIFICATION OF THE SMALL INTESTINAL SUBMUCOSA USING PLGA NANOPARTICLES FOR ENHANCED TISSUE REGENERATION: FROM *IN VITRO* TO *IN VIVO* MODELS

A DISSERTATION

SUBMITTED TO THE GRADUATE FACULTY

in partial fulfillment of the requirements for the

Degree of

DOCTOR OF PHILOSOPHY

By

FADEE G. MONDALEK
Norman, Oklahoma
2009

MODIFICATION OF THE SMALL INTESTINAL SUBMUCOSA
USING PLGA NANOPARTICLES FOR ENHANCED TISSUE REGENERATION:
FROM *IN VITRO* TO *IN VIVO* MODELS

A DISSERTATION APPROVED FOR THE
DEPARTMENT OF CHEMICAL, BIOLOGICAL AND MATERIALS ENGINEERING

BY

_____
Dr. Brian Grady, Chair

_____
Dr. Hsueh-Kung Lin

_____
Dr. Peter McFetridge

_____
Dr. Siribhinya Benyajati

_____
Dr. Chuanbin Mao

Acknowledgements

First I want to thank my wife, Amber, for standing by my side and supporting me at all times. In addition, I like to thank my family, friends, professors and fellow students for their continuous feedback especially Mr. Nabeel Shakir from the University of Oklahoma.

Special thanks go to Dr. Sundar Madihally and his graduate student Benjamin Lawrence (Department of Chemical Engineering, Oklahoma State University) for all their help and input on the SEM images and the permeability studies.

I wish to acknowledge Dr. Mike Ihnat (Department of Cell Biology, University of Oklahoma Health Sciences Center [OUHSC]) for providing the facility for conducting the CAM assay.

A big hand of appreciation goes to Dr. Kar-Ming Fung (Department of Pathology [OUHSC] and Department of Veterans Affairs Medical Center) for all his technical help on and analysis of immunohistochemical staining. We could not have done it without Dr. Fung. Special thanks to Drs. Andy Schultz, Blake Palmer, Christopher Roth, Yusuf Kibar and Richard Ashley for all their help with the animal surgeries.

Thanks to all my committee members for their constant feedback and suggestions: Dr. Siribhinya Benyajati (Department of Physiology, OUHSC), Drs. Brian Grady and Pete McFetridge (Department of Chemical, Biological, & Materials Engineering, University of Oklahoma) and Dr. Chuanbin Mao (Department of Chemistry and Biochemistry, University of Oklahoma).

Finally yet importantly, I like to thank Dr. Hsueh-Kung Lin (Department of Urology, OUHSC), my mentor and advisor, who supported me in every step in this project. Dr. Lin advised me continuously on several issues, in science as well as in life, and showed me the way to become a real scientist. He endured a lot during my quest and for all that, I am very grateful.

Table of Contents

List of Tables

List of Illustrations

Abstract

Small intestinal submucosa (SIS) derived from porcine small intestine has been intensively studied for its capacity in repairing and regenerating wounded and dysfunctional tissues. However, SIS suffers from a large spectrum of heterogeneity in microarchitecture leading to inconsistent results. The goal of this study is to modify an already existing SIS biomaterial with poly(lactide-co-glycolide) nanoparticles (PLGA NPs) for better tissue regeneration.

Specifically, nanoparticles made from PLGA were introduced into the SIS with the intention of decreasing the heterogeneity and improving the regenerative capability of this biomaterial. As determined by scanning electron microscopy and urea permeability, the optimum NP size was estimated to be between 200-500 nm. The PLGA NPs embedded in the SIS reduced the permeability of SIS to urea by almost 2-fold and did not change the tensile properties of the modified SIS as compared to the native SIS. More importantly, PLGA NP modified SIS did not affect human microvascular endothelial cells (HMEC-1) morphology or adhesion, but actually enhanced their growth.

These NPs were also used to deliver hyaluronic acid (HA) to enhance the angiogenic potential of SIS. Hyaluronic acid is an essential part of the extracellular matrix (ECM). HA in biomaterials has been shown to help improve tissue regeneration and enhance angiogenesis. To target optimal delivery of exogenous HA, an understanding of the expression of HA and its receptors in regenerated rat bladder was investigated. Our studies indicate that expression of HA and HA receptors, CD44 and LYVE-1, were not detected in rat bladder augmented with SIS until day 28 post-augmentation and thereafter.

HA-PLGA NPs were formulated to reduce the porous structure of SIS. Elevated cell proliferation was observed in HMEC-1 cells treated with HA-PLGA NPs as well as in HA-PLGA modified SIS (HA-PLGA-SIS). The HA-PLGA-SIS exhibited significantly enhanced neo-vascularization in an in ovo chorioallantoic membrane (CAM) angiogenesis model. The regenerative capability of the newly fabricated HA-PLGA-SIS was tested in a large animal bladder augmentation model. Bladders regenerated with HA-PLGA-SIS had significantly higher vascular ingrowth as compared to unmodified SIS. Based on the consensus that angiogenesis is essential for tissue regeneration, HA-PLGA-SIS represents a new approach for modifying naturally derived biomaterials in regenerative medicine.

Introduction

Organization of Thesis

Chapter 1 presents a detailed literature review on the subject matter. This chapter depicts the problem being addressed and discusses other research done in the field.

Chapter 2 describes the modification of an already existing biomaterial, small intestinal submucosa (SIS), with biodegradable polymer nanoparticles. Commercially available latex beads were used to determine the optimal size of the polymer nanoparticles that needed to be manufactured. The modified biomaterial was tested for its ability to support and sustain cell growth. The effects of the modification on the mechanical and physical properties of the SIS were also tested.

Chapter 3 describes the immunohistochemical staining for hyaluronic acid and its receptors in regenerated rat bladder augmented with SIS. These experiments showed how expression changed with different stages of the tissue regeneration as the wound healing process progressed. The understanding of this process was critical for the delivery timeline of exogenous hyaluronic acid to a biomaterial for the purpose of better tissue regeneration.

Chapter 4 describes how the biomaterial was modified with hyaluronic acid- polymer nanoparticles and the different characterization tests that were carried out. From *in vitro* experiments to large animal model studies, the HA-PLGA-SIS demonstrated its potential as the biomaterial to enhance tissue engineering.

Chapter 5 gives an overall conclusion of the project and draws a map for future experimentation.

Chapter 1 Background

Organ transplantation is a very important medical procedure, saving hundreds of thousands of lives each year. However, there is a severe shortage of donor tissues and organs, which is worsening every year given the aging population. Tissue engineering aiming at the construction of neo-tissues *in vitr*o or *in vivo* has become an attractive alternative to organ transplantation. Tissue engineering is defined as "an interdisciplinary field that applies the principles of engineering and life sciences towards the development of biological substitutes that aim to maintain, restore, or improve tissue function[1]." Tissue engineering has generated many promising results. The selection of biomaterials as scaffolds is a critical factor in determining the success of tissue regeneration in the field of tissue engineering.

Tissue engineering in bladder regeneration

The main function of the bladder is to store urine at a safe pressure for the kidneys to operate normally and empty it in an acceptable manner[2]. There are several conditions that can lead to bladder disorders and malfunction, some of which are trauma, inflammation, disease, radiation and cancer. Loss of bladder function can lead to renal failure and urinary tract infection[2]. Patients that undergo partial cystectomy require bladder tissue replacement to restore bladder function. Bladder reconstruction has been used as a surgical procedure for treating a wide range of congenital and acquired diseases[3,4].

When pharmacological treatment and intermittent catheterization fail, bladder augmentation is needed and involves removing the top portion of the bladder dome and replacing it with gastrointestinal segments from the same patient (autogenous tissue) to

eliminate any immune response. Today, cystoplasty using the ileum, colon, or stomach segments is the gold standard procedure for bladder augmentation[2]. Unfortunately, the use of gastrointestinal segments for bladder augmentation can lead to electrolyte imbalance, stone formation, excessive mucus production, urinary tract infection, bacterial colonization, and cancer. Gurocak et al. did an excellent job providing a review of the current state of bladder augmentation technology[5]. The goal of having an off-the-shelf biomaterial with no complications has not yet been achieved. Hence, bladder wall replacement is one of the most challenging problems in urologic surgery.

The major obstacle to advancing the field of urinary tract reconstruction and rehabilitation has been the availability of a biomaterial, either permanent or biodegradable, that will function as a suitable scaffold to allow the natural process of regeneration to occur. The ideal graft material would promote the development of a structurally intact low-pressure reservoir, serve as a scaffold for the healing and regeneration of the bladder wall, and ultimately be replaced by the host tissue. If a suitable exogenous graft material was available, the need for autogenous tissue and all of the negative consequences associated with it could be eliminated. Therefore, investigators continue to search for the proper scaffold and methodology that is necessary to regenerate tissue and maximally restore urinary tract function. Currently, two technologies involving tissue engineering for bladder regeneration and augmentation are being investigated.

The first reconstructive technology, the *in vivo* or unseeded tissue engineering technique for bladder regeneration, employs xenogenic (derived from stomach, bladder and small intestine) or synthetic biodegradable, acellular matrices. Such tissue engineering technique involves the direct *in vivo* placement of an unseeded biodegradable

material into a host that will then function as a scaffold to allow the natural process of regeneration to occur. While this technology provides the scaffold for wound healing and tissue regeneration, it also requires the host to provide the tissue and proper environment for cell growth and tissue regeneration. There are two major obstacles for this unseeded tissue engineering technology for bladder regeneration. The first has been finding a biomaterial that will act as a suitable scaffold for this natural process to occur. Synthetic non-biodegradable biomaterials such as silicone, rubber, polytetrafluoroethylene and polypropylene have been unsuccessful because of mechanical failure, lithogenesis, or host-foreign body reactions[6-8].

As a consequence of failures with non-biodegradable materials, synthetic and natural biodegradable materials have been investigated that would allow the host bladder time for regeneration but then dissolve prior to the onset of any foreign body reaction. These materials have shown improvements over non-biodegradable materials. Xenogenic, collagen-rich biodegradable materials such as placenta, amnion and pericardium have been used with even more encouraging experimental results than studies employing non-biodegradable synthetic materials. However, despite initial encouraging results, none of these materials has been found to be suitable for clinical use. It has been reported that bladders augmented with dura, peritoneum, placenta and fascia contracted over time, and that such tissue grafts failed to promote a complete bladder wall regeneration[9]. Synthetic biodegradable polymers such as polyglycolic acid (PGA), polylactic acid (PLA), or poly(lactide-co-glycolide) (PLGA) have also been studied for bladder augmentation due to their structural and mechanical properties[10,11]. Most of these matrices also cause

complications such as lithiasis formation, infections, graft rejection, extrusion, or failure to adequately regenerate a full bladder[12].

Optimal materials need to be developed to provide the "perfect" biomaterial for appropriate tissue regeneration. The creation of hybrid materials from synthetic and natural substrates is an emerging filed in tissue engineering. It combines the biologic activities of naturally derived materials with favorable properties of synthetic ones such as mechanical properties and consistent reproducibility.

Therefore, the design of synthetic bioscaffolds has shifted from strictly using synthetic polymers to combining these polymers with other biomaterials and molecules to enhance tissue engineering. Nakanishi et al. showed that a PLGA mesh-collagen hybrid scaffold seeded with urothelial and smooth muscle cells can been used to reconstruct a three-dimensional urinary bladder wall[13]. Oh's group incorporated calcium peroxide-based oxygen generating particles into PLGA scaffolds and showed that this new material can extend cell viability under hypoxic conditions[14]. Even though scaffolds made with synthetic and natural components have shown promising regenerative results, we do not yet have an off-the-shelf biomaterial that has been optimized for tissue engineering.

The second potential limitation of the unseeded tissue engineering technique for bladder regeneration is that the size of the graft may be limited to the size of area that needs regeneration, which can be quickly occupied with bladder cells from the remaining native bladder. If the ratio of the size of the unseeded graft to the amount of remaining native bladder tissue becomes too large, the ability of the body to occupy the graft with smooth muscle and urothelial cells appears to be compromised. In the absence of quickly covering the graft with bladder cells, contraction and excess scar formation becomes a

concern and poor clinical outcomes may result. Clearly a tissue graft material is desired which is non-immunogenic, not subject to gross shrinkage after implantation, and which promotes the growth of endogenous urinary bladder tissues having a urine impermeable cell layer and a functional smooth muscle cell layer.

The second tissue reconstruction technology, the *in vitro* or seeded tissue engineering technique, utilizes biodegradable materials that serve as both a scaffold for the regeneration process to occur as well as cell-delivery vehicles. This technology involves initial harvesting of bladder tissue, such as from a biopsy from host native tissue, to establish primary cultures of bladder cells. Cilento et al. demonstrated that it is theoretically possible to expand a transitional epithelial strain to cover the area of an entire football field using this method of cell culture[15]. These cells are then seeded on a biodegradable membrane and, following a period of graft maturation, the *in vitro* created bladder graft is then transplanted back into the host for continuation of the regeneration process. Yoo et al[16] and Oberpenning et al[17] reported on the feasibility of dog bladder augmentation using allogenic bladder submucosa and polyglycolic acid polymers membranes seeded with urothelial and smooth muscle cells. This study demonstrated that transitional epithelium and smooth muscle cells could be harvested, grown and subsequently seeded on allogenic bladder submucosa for use as augmentation material. Urodynamically, the augmented bladder demonstrated increased capacity during this short-term study. Interestingly, the unseeded allogenic bladder submucosa also demonstrated the ability to increase bladder capacity; however, the gains in capacity were less than the seeded grafts.

Recently in 2006, Atala et al. performed a study where seven patients, ages 4-19 years old, had their bladders augmented with a bladder-shaped scaffold made of a composite of collagen and PGA seeded with patients' urothelial and smooth muscle cells that have been grown in culture[11]. The follow-up period was 22-61 months (mean 46 months). Bowel function returned promptly after surgery. No complications were observed. The engineered bladder showed an adequate structural architecture and phenotype. They concluded that collagen-PGA scaffolds seeded with cells obtained from the patients and wrapped with omentum could be used in patients needing cystoplasty.

Studies such as these suggest that prior cell seeding of large bladder grafts may be necessary to obtain the best clinical outcome following bladder augmentation. Unfortunately, although the *in vitro* technique of tissue engineering has been shown to be feasible for both synthetic and xenogenic matrices, there is still a risk of obtaining unhealthy cells from the patients to put on the scaffold. Therefore, having a cell-seeded off-the-shelf biomaterial is not practically desirable. In the present study, we have decided to go with the unseeded technology and used small intestinal submucosa (SIS) as the scaffold of choice.

Small intestinal submucosa in tissue engineering

SIS is a xenogenic membrane harvested from porcine small intestine in which the tunica mucosa and the serosa muscularis are

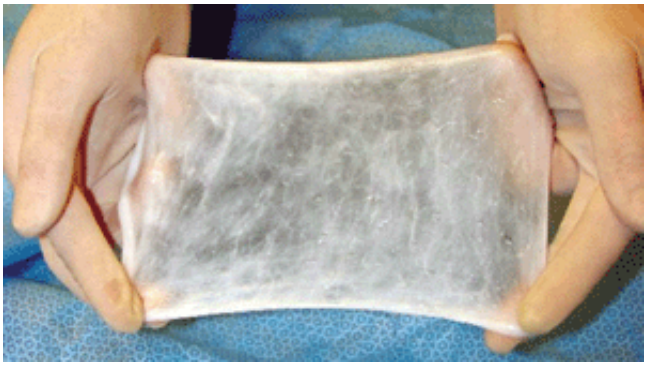

Figure 1-1 Small intestinal submucosa (SIS)

mechanically removed from the inner and outer intestine respectively, producing a thin, translucent graft (0.1 mm wall thickness) composed mainly of the submucosal layer of the intestinal wall[18] (Figure 1-1). The submucosal layer of animal intestine has an established background in surgery as gut suture. SIS has been used successfully to repair and replace a variety of tissues including tendon[19], arterial and venous tissues[20,21], skin[22], abdominal wall[23] and bladder[24,25] in various animal models from rodents[26] to rabbits[27] to dogs[28]. SIS is one of the most thoroughly studied collagen-based naturally occurring biomaterials for urinary tract reconstruction including ureter, bladder, and urethra[29-34]. The tremendous success of SIS is attributed to the fact that SIS contains an endogenous mixture of active intrinsic growth factors[35], cytokines, structural proteins, glycoproteins and proteoglycans[36] that may assist in cell migration, cell to cell interaction, and cell growth and differentiation during the regenerative process[37].

Researchers have shown that SIS can successfully regenerate a functional bladder in animal models[29-31]. When SIS was used for urinary bladder augmentations in the rat, rabbit, and dog models, it was demonstrated that the SIS functioned as a scaffold allowing the native bladder to remodel and regenerate itself. Histologically, the regenerated bladder contained transitional epithelium, smooth muscle, as well as peripheral nerves and were indistinguishable from the normal bladder in long-term augmentation studies[29,32].

However, there have been contradicting results throughout the literature about the outcome results of SIS usage. Petter-Puchner et al showed that the SIS showed adverse effects when used for ventral hernia repair in rats[38]. These effects included severe local reaction around SIS at time of harvesting causing inability to perform biomechanical

testing. They concluded that further investigation needed to be done before clinical use of SIS in hernia repair. On the other hand, in a 3-year follow-up study performed in seventy male patients, Ansaloni's group compared SIS with polypropylene mesh for inguinal hernia repair[39]. They devised a scaling system to quantify the results and showed that using the SIS in a clinical trial was safe and effective.

To date, SIS has been shown to be non-immunogenic in over 1,000 cross-species transplants and direct challenge testing, demonstrating the lack of immunogenicity thereof. Kropp et al. performed urinary bladder augmentation in a rat model using SIS, and showed that SIS functions as a scaffold that allows the native rat bladder to remodel and regenerate itself[40]. Histologically, the regenerated rat bladders contained all three layers of the bladder (urothelium, smooth muscle and serosa) and were indistinguishable from normal rat bladder at 11 months post-augmentation. In addition, *in vitro* contractility studies showed that strips of *in vivo* tissue engineered SIS-regenerated rat bladder had contractile properties and nerve regeneration that was similar to the normal rat bladder[41]. This was the first evidence that a functional bladder could be achieved with tissue engineering techniques using SIS. It also demonstrated that SIS was different from other biomaterials that have been studied in the past. Previously, no other material had shown the ability to promote the regenerative capacity of bladder tissue that SIS demonstrated in the small animal model.

In spite of the advantages and success of the SIS, researchers could not produce consistent bladder regeneration despite using the same techniques. It is not fully understood what causes this inconsistency in regeneration. One possibility is variations in the way SIS is manufactured and processed. Kropp et al. were the first group to discover

and publish that the regenerative property of SIS is location-dependent[42]. Distal SIS hat is taken from the ileum close to the ileocecal valve shows consistently excellent regenerative properties. On the other hand, SIS made from the proximal jejunum (proximal SIS) produces poor bladder regeneration with scar formation and graft shrinkage. That group also showed that the physical properties of SIS are also location-dependent[43].

In addition, while all segments of small intestinal submucosa have been used to promote urinary bladder regeneration, multiple problems have been encountered with different small intestinal segments, including calcifications and graft shrinkage, and therefore unreliable and inconsistent results have been obtained in the experimental use of this material for bladder augmentation. However, no studies have previously been undertaken to determine if SIS can be modified to provide a uniform structure or modified to incorporate macromolecules that are important for tissue regeneration and thus enhance the tissue engineering process.

As discussed earlier, SIS has limited regeneration capability especially in large size graft tissue. If the seeded technology is not desirable, then the unseeded technique must be improved. One approach is to enhance the angiogenic capability of the SIS. Therefore, there is a need within the tissue engineering field to identify new and improved tissue graft substrates that have a substantially uniform structure that can deliver macromolecules for enhanced angiogenic effect. These biomaterials have to enhance the regeneration process through angiogenesis and generate reliable and reproducible results, thereby overcoming the disadvantages and defects of the prior technologies. Therefore,

this study focused on modification of the SIS using poly(lactide-co-glycolide) nanoparticles to enhance the angiogenic potential and regenerative capability of the SIS.

Poly(lactide-co-glycolide) nanoparticles for delivery of macromolecules

Nanotechnology involves the formulation and manipulation of materials to create unique products with novel properties at the nanoscale level. Nanoparticles (NPs) are submicron-sized polymeric colloids, and have been designed to deliver biologic molecules of interest either encapsulated within or condensed/conjugated on the surface of the particles[44]. Synthetic polymers have been used for manufacturing nanoparticles. Nanoparticles made from PGA, PLA and their copolymers (PLGA) represents a new generation of delivery systems. These synthetic biodegradable polymers are non-toxic, do not elicit an immune response, biocompatible, biodegradable, and are approved by the Food and Drug Administration (FDA) for clinical usages[45]. Poly(lactide-co-glycolide) or PLGA is the most studied synthetic polymer based on the properties stated above. PLGA nanoparticles have been intensively investigated as potential carriers for macromolecules such as drugs[46-50], genes[51-56] and hormones[57]. They have been used as anti-cancer treatments[58-60] and as diagnosis tools[61].

Nanoparticles are advantageous over larger systems because they operate at the size scale of proteins giving them the ability for cell interaction and communication through the nanoscale environment. They are small enough to be internalized into arteries[46] or cells[62] if needed. PLGA nanoparticles can improve the compatibility of macromolecules used for therapeutic purposes; and the release rates of the biological macromolecules can be regulated by controlling the degradation rate of the nanoparticles.

There are two methods to formulate NPs. The first is the “bottom up” method and the second is referred to as the “top down”. In the first procedure, the individual monomers or building blocks are precisely engineered and the nanoparticles are produced through self-assembly[63,64]. Very few researchers use this method for the manufacture of NPs. This process is tedious and time consuming which makes it uncommon and not preferred by nanoparticle scientists.

In the “top down” method, as the name implies, the process starts with large sizes of polymer and gradually reducing the size using different physical/chemical techniques. This is the most common procedure used to make NPs. Different procedures are available to formulate PLGA NPs. Astete and Sabliov provide a detailed review covering this issue[65]. The physical characteristics of PLGA NPs (size, size distribution, morphology, zeta potential) are affected by the different manufacturing methods as well as synthesis parameters. Below is a brief description of the two common methods used. These methods apply to other polymers but we will focus on PLGA.

Emulsion diffusion method: in this method, PLGA is dissolved in an organic solvent that should be partially miscible with water such as ethyl acetate[66]. The organic phase is emulsified with an aqueous solution containing a suitable surfactant such as polyvinyl alcohol (PVA) under continuous stirring. The diffusion of the organic solvent and the counter diffusion of water into the emulsion droplets is what cause the formation of the NPs[67]. Many parameters affect the NPs size including: PLGA monomer ratio (PLA:PGA), PLGA concentration and molecular weight (MW), organic solvent used, viscosity, organic and aqueous phase ratios, temperature, mixing rate, surfactant used and its ratio to the polymer, and the rate at which the aqueous phase is added.

This method is used for encapsulating hydrophobic compounds. It does not require high-energy consumption because it requires mild stirring. It does not use any toxic solvents. Common disadvantages include low entrapment efficiency of hydrophilic compounds (most drugs are hydrophilic), use of large volume of water for NPs formulation and large time of emulsion agitation.

Emulsion evaporation method: this is the oldest method used to make NPs. PLGA is dissolved in an organic solvent such as chloroform or methylene chloride. The organic phase is poured into the aqueous phase containing a surfactant and emulsified under high shear stress. The final step involves the evaporation of the organic solvent under vacuum inducing the formation of NPs. This is referred to as the oil in water (o/w) emulsion[68]. The water in oil (w/o) emulsion requires pouring the aqueous phase into the organic phase containing a surfactant and emulsifying[69]. Both w/o and o/w are referred to as single emulsions. The water in oil in water (w/o/w), also called double emulsion, involves the same steps of making a w/o emulsion. An additional step is pouring that w/o emulsion in a large volume of water under high shear stress and evaporating the organic solvent under vacuum[70]. Parameters that need to be considered are PLGA concentration and MW, surfactant used, PLA:PGA ratio, organic to aqueous phases' ratio, evaporation rate and shear stress.

The o/w emulsion is used for the entrapment of hydrophobic components, whereas the w/o/w emulsion is used for hydrophilic components. This method is widely used because it is easy to scale up. It uses non-toxic solvents. Additives can be used to reduce the NPs size. The main drawback of this process is the use of high shear stress such as sonication.

There is a lot of room for modification considering that many parameters, such as PLGA concentration, MW, monomer ratio and so forth, can affect the physical characteristics of the NPs. For example, changing the percentage of surfactant/stabilizer in the aqueous phase of the second emulsion affects the size of the nanoparticles. Changing the monomer ratio of PLA and PGA changes the degradation rate of the PLGA nanoparticles and hence affects the release rate of encapsulated molecules within the nanoparticles. For example, PGA is hydrophobic while PLA is hydrophilic. Therefore, the higher the PGA content in PLGA, the more hydrophobic the nanoparticles are and the slower is their degradation. The exception to that rule is the 50:50 ratio, which degrades the fastest. We chose to use the emulsion evaporation method to make NPs because it allows us to adjust the characteristics of the NPs.

Angiogenesis in tissue repair and regeneration

Angiogenesis, the formation of new blood vessels from pre-existing ones, is essential in tissue and organ regeneration to provide a continuous support of nutrients and oxygen as well as carrying away waste byproducts[71]. Angiogenesis depends on the dynamic interactions between cytokines, the extracellular matrix (ECM), smooth muscle cells and endothelial cells. Impaired angiogenesis leads to impaired wound healing[72]; and improved wound healing is observed after topical administration of growth factors, particularly angiogenic factors[73].

The formation of blood vessels during the embryologic stage, vasculogenesis and angiogenesis, are the responsible processes for building the adequate vasculature to transport oxygen and nutrients in normal and pathologic stages. Disruption of one of these processes may result in lethal anatomical abnormalities[74,75]. Throughout the last two

decades, tissue engineering has proposed strategies to generate tissues in the laboratory in order to replace lost or malfunctioning organs. This endeavor has been proven extremely challenging due to the inability of the vascular network to penetrate into deeper layers of the new tissue. It is well known that cells more than a few hundred microns from a blood vessel will not survive due to diffusion limitations. This inability to develop the appropriate vascular supply to *in vitro* generated tissues has led to *in vitro* generated tissues of limited size.

The requirement of a rapid, complete and organized formation of a blood vascular network for successful wound healing and tissue regeneration has also been demonstrated in other clinical settings. For example, free skin grafts survive only if they are placed in a healthy and vascularized stromal bed[76]. A variety of strategies using allografts, collagens, and other biological scaffolds have been designed to enhance blood vessel ingrowth into the regenerating tissues[77-81]. To improve angiogenesis for successful tissue regeneration, angiogenic factors such as vascular endothelial growth factor (VEGF)[82] have been genetically introduced into cells seeded onto biodegradable grafts to enhance host blood vessels ingrowth into engineered tissues. Exogenous HA has also been introduced into scaffolds and shown to enhance angiogenesis[83].

Angiogenesis has been widely studied in the context of several pathologies such as inflammation, tumor growth, rheumatoid arthritis, wound healing and diabetic retinopathy because in theory, manipulating the vascular growth could be an effective strategy to control these pathologies. Angiogenesis is controlled by angiogenic factors (AF), which are substances that participate in directing organ development, and to date several substances have been identified. These include the vascular endothelial growth

factor (VEGF) family[84-87], the fibroblast growth factor (FGF) family[88], the transforming growth factor (TGF-α and TGF-ß)[89], platelet derived growth factor (PDGF)[90], tumor necrosis factor alpha (TNF-α)[91,92], angiopoietins[93-95], interleukins[96], leptin[97], and last but not least important, hyaluronic acid (HA) derivatives[98].

Oxygen and nutrients are necessary for the growth, maintenance and reproduction of cells, tissues and organs under normal or pathologic conditions. During wound healing and tissue regeneration, the delivery of oxygen and nutrients is of critical importance for rebuilding a given organ. Oxygen generating scaffolds have been shown to extend cell viability under hypoxic conditions[14]. These biomaterials may allow for increased cell survival while angiogenesis is being established.

When it comes to studying a pro-angiogenic molecule for a specific application, it is hard to make a choice given the multiple angiogenic factors that have been identified so far and the vast array of research done to date. Would you pick one molecule of choice or a combination of two or more? Many molecules in our body have overlapping roles or signaling pathways. It is very difficult and sometimes nearly impossible to study the effect of a single factor in complete isolation of its environment. However, one thing is for sure, angiogenic factors are needed to stimulate new blood vessel formation, which in turn enhances tissue regeneration.

The work carried out on VEGF, which is implicated in the differentiation, migration and proliferation of endothelial cells, is extensive including more than a thousand papers for the biology of this molecule[99]. This protein is recognized as one of the most potent AF and there are several isoforms; three of these, $VEGF^{121}$, $VEGF^{165}$ and $VEGF^{189}$ are the most widely studied. However, although VEGF treatment remains promising for

enhancing angiogenesis, results have been somewhat disappointing and there are still several drawbacks to be overcome. For instance, there is an uncertainty about which delivery route to take, the speed of administration and the appropriate dosage. Furthermore, it is very well known that VEGF is also a potent vascular permeabilizing factor hence the first name for VEGF was vascular permeability factor (VPF)[84,100]. The most common collateral effect seen in pathologic stages and clinical trials has been the increase of blood vessel permeability[101,102], which leads to fluid and proteins extravasations (e.g., fibrin deposits) and edema formation[103-105]. On the other hand, endothelial cells are not the only cells stimulated by this cytokine; lymphatic vasculature has also been stimulated by members of the VEGF family[106,107]. These findings have triggered the search for new molecules as alternatives when angiogenesis induction is considered as a treatment.

Hyaluronic acid

Hyaluronic acid (hyaluronan, sodium hyaluronate, HA) is a member of the glycosaminoglycans (GAGs) family, which are found almost exclusively in animals and primarily used to give structural stability to the tissues. GAGs are a family of naturally occurring linear or branched, negatively charged polymers. Other members of this family include dermatan sulfate, chondroitin sulfate, heparan sulfate, heparin, and keratan sulfate. HA is the only member of this family that is found non-sulphated, and not covalently bound to proteins. It has a molecular weight that ranges from 412 Da to 2×10^4 kDa. HA is a natural polysaccharide composed of alternating (1 $\rightarrow$ 4)-β linked glucouronic acid and (1 $\rightarrow$ 3)-β linked N-acetyl-$_D$-glucosamine (Figure 1-2).

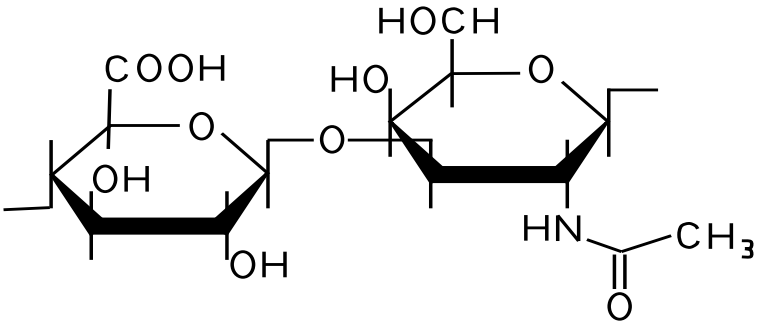

Figure 1-2 Chemical structure of hyaluronic acid

HA was first identified when Meyer and Palmer isolated it from the vitreous humor of bovine eyes in 1934[108]. The name was derived from *hyalos*, which is Greek for vitreous. In mammals, It is found in heart valves, skeletal tissue, umbilical cord, vitreous of the eye, synovial fluid and skin[109]. It is also an important part of the ECM because of its large molecular weight-space filling feature[110]. This large molecule is negatively charged hence attracting positive ions creating an osmotic imbalance that draws in water. HA has the capacity of binding huge amounts of water almost one thousand times its own weight giving it the ability to function as a biological lubricant in joints[109]. Table 1-1 shows common abundances of HA in animal tissues[110].

HA synthesis in the body is carried out by membrane-bound HA synthases (HAS), namely HAS1, HAS2 and HAS3. HA is unique among matrix macromolecules because it is directly secreted into the ECM as it is synthesized by smooth muscle cells[111]. These synthases produce different chain length HA. HAS1 and HAS2 produce HA of 2×10^5-2×10^6 Da, whereas HAS3 produces HA of 1×10^5-1×10^6 Da, although this can vary depending on cell type[112].

Table 1-1 Occurrences of HA in animal tissues

Tissue or body fluid	Concentration (μg/ml)	Remarks
Rooster comb	7500	The animal tissue with by far the highest HA content
Human umbilical cord	4100	Contains primarily HA with a relatively high molar mass
Human joint fluid (SF)	1400-3600	The volume of SF increases under inflammatory conditions. This leads to a decreased HA concentration
Bovine nasal cartilage	1200	Often used as a cartilage model in experimental studies
Human vitreous body	140-340	HA concentration increases upon the maturation of this tissue
Human dermis	200-500	Suggested as a “rejuvenating” agent in cosmetic dermatology
Human epidermis	100	HA concentration is much higher around the cells that synthesize HA
Rabbit brain	65	HA is supposed to reduce the probability of occurrence of brain tumors
Rabbit heart	27	HA is a major constituent in the pathological matrix that occludes the artery in coronary restenosis
Human thoracic lymph	0.2-50	The low molar mass of this HA is explained by the preferential uptake of the larger molecules by the liver endothelial cells
Human urine	0.1-0.3	Urine is also an important source of hyalurodinase
Human serum	0.01-0.1	HA concentrations increase in serum from elderly people as well as in patients with rheumatoid arthritis and liver cirrhosis

A wide range of cellular activities requires HA such as cell migration, cell-cell adhesion, cell differentiation[113], cell proliferation[114], morphogenesis[115], inflammation[116] and angiogenesis[117]. HA has some unique viscoelastic and rheological properties that make it play an important physiological role in living organisms and an attractive

biomaterial for medical applications[110]. The biomedical applications of HA as Balazs states it are as follows[118]:

1. Viscosurgery: protect delicate tissue and provide space during surgical manipulations such as eye surgery.
2. Viscoaugmentation: fill and augment tissue spaces such as skin and vocal tissues.
3. Viscoseparation: separate connective tissue to prevent adhesions and scar formations during wound healing.
4. Viscosupplementation: replace tissue fluids such as synovial fluid and relieve pain.

HA is degraded by a group of enzymes called hyalurodinases (HYALs)[109]. These enzymes degrade the (1 $\rightarrow$ 4)-β linkage between N-acetyl glucosamine and glucouronic acid. There are six hyalurodinases: HYAL1-4, PH20 and HYALP1[109]. HYAL1 is the major hyalurodinase in plasma and urine that degrades HA extracellularly because it is active at physiologic pH[119]. HYAL2 is a cell surface enzyme that degrades only high molecular weight HA to fragments about 20 kDa, which are further degraded into smaller fragments by PH20[109]. PH20 is important during egg fertilization by sperm as it is located on the surface of sperm[119]. HYAL3 expresses in testis sand bone marrow and has no hyalurodinase activity[109]. HYAL4 is restricted to placenta and skeletal muscle and similar to HYAL3 has no hyalurodinase activity[119]. Not much is known about HYALP1.

HA has been intensively studied for its involvement in wound healing processes. HA has been shown to modulate inflammatory responses in several ways to reduce scarring by directly promoting fibroblast migration, protecting cells against free radical damage,

influencing both the amount and nature of collagen production, and forming a matrix that binds protein inhibitors of serine proteinases such as plasmin, cathepsin G, and activators of matrix metalloproteinases[111]. Below is a summary of the biological effects of HA in the wound healing process (Table 1-2)[111].

Table 1-2 Biological functions of HA in the wound healing process

Stage	**Process**	**Mechanism**
Inflammatory phase	Inflammation activation	Enhancement of cell infiltration Increase of pro-inflammatory cytokines TNF-α, IL-1β and IL-8 via a CD44 mediated mechanism Facilitates primary adhesion of cytokine-activated lymphocytes to endothelium
	Inflammation moderation	Free radical scavenging and antioxidant properties TSG-6 and IαI mediated inhibition of inflammatory proteinases
Granulation phase	Cell proliferation	HA synthesis facilitates cell detachment and mitosis
	Cell migration	Increased HA synthesis HA-rich granulation tissue provides open, hydrated matrix that facilitates cell migration Receptor mediated cell migration, e.g. CD44, RHAMM
	Angiogenesis	Angiogenic properties of low MW HA oligosaccharides
Re-epithelialization	Keratinocyte functions	HA-rich matrix is associated with proliferating basal keratinocytes Facilitates keratinocyte migration via a CD44 mediated mechanism
Remodeling	Scarring	HA-rich matrix may reduce collagen deposition, leading to reduced scarring as seen in fetal wound healing

Delivery of exogenous HA has been shown to produce beneficial wound healing outcome. Application of HA topically on rat skin wounds have shown to accelerate the wound healing process[120]. It is believed HA has a major effect on events leading to the fetal scarless wound healing[121]. HA content in fetal wounds remains higher and for prolonged periods of time compared to adult wounds suggesting HA's role in reducing collagen deposition and hence reducing scarring[122]. This is in agreement with the work of Laurent et al. who showed that applying HA to tympanic membranes of rats resulted in scarless wound healing[123].

HA's complete lack of immunogenicity, widespread availability and ease of chain size manipulation make it an ideal material for designing novel drug delivery systems. HA-based or HA-hybrid scaffolds have been applied in the field of tissue engineering and have been shown to be promising biomaterials for improving angiogenesis and tissue regeneration[124,125]. HA is also an FDA approved product for clinical applications to improve organ repair and function as well as for cosmetic applications.

When fractionated by enzymatic digestion with hyalurodinase, fragments in the range of 4 to 24 disaccharides were shown to be angiogenic on the chorioallantoic membrane (CAM) model[98]. This study exposed the possibility of a dual effect of HA on blood vessel formation: long chains are anti-angiogenic whereas small fragments are pro-angiogenic[126]. Table 1-3 lists some of the size-related functions of HA[127]. Other studies have shown similar conflicting results; for instance, oligosaccharides of HA (o-HA), were implicated in angiogenesis when wound-drainage fluid obtained from healthy and pathologic humans were tested for blood vessel development on the CAM model. The fluid extracted from wounds and applied directly on the CAM without any previous

processing was rich in high MW HA and did not show any changes. On the other hand, when the extracted fluid was treated with hyalurodinase, which degrades HA into smaller fragments or o-HA, neovascularization was observed. This confirmed the opposite effects of different sizes of HA in the wound extract[128-130].

Table 1-3 Sizes of HA with key functions

Size (saccharides)	**Function**
Native or high MW (HA>1000-5000)	Suppression of angiogenesis Immune suppression Inhibition of phagocytosis Suppression of HA synthesis
HA fragments (~ 1000)	Induction of inflammatory chemokines Stimulation of PAI-1 Stimulation of urokinase
10-40	Induction of CD44 cleavage Promotion of tumor cell migration
8-32	Stimulation of angiogenesis Stimulation of tumor neovascularization
~ 15	Suppression of smooth muscle cell proliferation
12	Endothelial cell differentiation Upregulation of PTEN in tumor cells
10	Displacement of matrix HA on oocyte surface Displacement of proteoglycans from cell surface
6	Suppressions of HA cable formation Induction of NO and MMPs in chondrocytes Induction of HAS2 in chondrocytes
4-6	Induction of cytokine synthesis in dendritic cells Transcription of MMPs
4	Upregulation of Hsp 72 expression Suppression of apoptosis Induction of chemotaxis Upregulation of heat shock factor-1 Upregulation of Fas expression Suppression of proteoglycan sulfation

New effects have also been described for o-HA, including for example, that intermediate sizes of o-HA (80 to 120 kDa) are implicated in the modulation of inflammation and immunologic responses[131,132] while sizes ranging from 2 to 3.5 kDa were found to cause apoptosis in some cancer cell lines[133,134]. This ubiquitous molecule has triggered the interest of researchers in several fields. For researchers in the oncology field, HA might be a molecule that can be used in the treatment of some types of cancer. For tissue engineers, it would be a means to create vasculature for tissue engineering purposes by blocking either the molecule or its receptors to control blood vessel development.

Research studies have demonstrated five hyaluronic acid receptors: CD44 (Cluster of Differentiation 44) also called Pgp-1 and H-CAM; LYVE-1 (Lymphatic Vessel Endothelial Receptor 1); HARE (HA Receptor for Endocytosis), also called LEC (Liver Endothelial Cell receptor); VEGFR-3 (Vascular Endothelial Growth Factor Receptor 3), and RHAMM (Receptor for HA Mediated Motility), also called IHABP (Intracellular HA Binding Protein). CD 44 is the major receptor for HA[135,136]. It also binds ligands other than HA. The binding of HA to CD44 has been shown to be involved in cell-cell and cell-ECM adhesion[137] as well as cell motility, endocytic uptake of HA, intracellular degradation of HA and ECM remodeling[138,139]. Studies in CD44 knockout mice show reduced ability to undergo normal would healing because of decreased cell migration, motility and ECM turnover[112].

The binding of HA to RHAMM is also involved in cell motility[140]. When the adhesion of HA to RHAMM has been blocked in mice, there was an inhibition of Fibroblast growth factor (FGF)-induced neovascularization[112]. HARE seems to be

involved in the clearance of HA from the blood and lymph[113,116]. LYVE-1 is expressed in lymphatic endothelial cells that bind HA in ECM and lymphatic fluid. LYVE-1 is believed to be involved in the transport of HA from tissue to distant lymph nodes for degradation[141,142]. The binding of HA to VEGFR-3 is not fully understood.

With this evidence, HA might provide significant assistance in developing a tissue engineering replacement of bladder sections using the PLGA NP modified SIS. We sought to deliver the HA to the SIS prior to *in vivo* experimentation by condensing the HA on the surface of the biodegradable PLGA NPs and gravity filter the whole complex (HA-PLGA NPs) through the SIS.

The problem continues

In summary, the SIS has shown great potential for tissue regeneration in many organs and tissues across multiple species. The SIS high permeability to urine and inability to support large size graft areas are still important issues that need to be addressed if clinical trials are to be conducted. We have sought to formulate PLGA NPs using the double emulsion technique and use these NPs to reduce the permeability of the SIS and as the delivery vehicle for HA. These HA-PLGA NPs are intended to modify the SIS and improve the angiogenic potential of this biomaterial through the continuous release of HA. The hypothesis is that if more blood vessels infiltrate the implanted tissue, the regeneration rate would improve, as nutrient mass transfer would be less limiting allowing more cells to be recruited to the area. Therefore, improved angiogenesis needs to be addressed if optimal results for tissue engineering are desired. Further, we hypothesize that this approach can be accomplished using the aforementioned PLGA NPs due to their capability of releasing therapeutic agents at sustained rates[65].

Chapter 2 The incorporation of poly(lactide-co-glycolide) nanoparticles into porcine small intestinal submucosa biomaterials and its properties

1. INTRODUCTION

Small intestinal submucosa (SIS) derived from porcine small intestine has been intensively studied for its capacity in repairing and regenerating wounded and dysfunctional tissues. However, SIS suffers from a large spectrum of heterogeneity in microarchitecture leading to inconsistent results. In this study, we introduced poly(lactide-co-glycolide) nanoparticles (PLGA NPs) to SIS with an intention of decreasing the heterogeneity and improving the consistency of this biomaterial. This modification in the SIS physical properties was tested by studying the permeability of the PLGA NPs modified SIS to urea, a common nitrogenous waste product in urine. We also tested the effect of this modification on the mechanical properties of the SIS and investigated the influence of the new biomaterial on endothelial cell growth.

2. MATERIALS AND METHODS

2.1 Materials

PLGA with a 50:50 monomer ratio, molecular weight of 106 kDa, and viscosity of 1.05 dl/g was purchased from Absorbable Polymers International (Pelham, AL). Negatively charged polystyrene latex spheres (six sizes between 50 and 2,000 nm), urea, poly(vinyl alcohol) [PVA], poly(ethyleneimine) [PEI], and endothelial cell culture medium (MCDB-131) were obtained from Sigma-Aldrich (St. Louis, MO). Single layer SIS (Surgisis®) was obtained from Cook® Biotech (West Lafayette, IN). Chloroform was purchased from EMD Chemicals (San Diego, CA). Urea assay kit was purchased from

Diagnostics Chemicals Limited (Oxford, CT). Fetal bovine serum (FBS) and penicillin-streptomycin were obtained from Invitrogen (Carlsbad, CA). Human microvascular endothelial cells (HMEC-1) were provided by Dr. Mike Ihnat at the University of Oklahoma Health Sciences Center[143].

2.2 Synthesis of PLGA NPs

PLGA NPs were synthesized using a modified double emulsion solvent evaporation technique[65]. Briefly, 30 mg of PLGA was first dissolved in 1 ml of chloroform. An aliquot of 200 µl of 7% PEI (used to produce positively charge nanoparticles) was added to the PLGA/chloroform solution followed by sonication on ice with a probe sonicator (model VC60; Sonics & Materials, Danbury, CT) set in a continuous mode for 30 seconds at 100% amplitude. The primary emulsion was transferred into 10 ml of 1% PVA; and the entire solution was sonicated on ice for another 1 min. The organic solvent in the final solution was allowed to evaporate overnight with continuous stirring. PLGA NPs were recovered by centrifugation at 30,000 × *g* for 20 min at 4^{o}C. The pellet consisting of aggregated NPs was washed three times with water to remove any residual PVA. PLGA NPs were then resuspended in water using sonication, freeze-dried and then stored at -20^{o}C for later use. The lyophilized NPs are stable up to six months at -20^{o}C.

2.3 Characterization of PLGA NPs

PLGA NPs were assessed for the particle size, polydispersity index, and zeta potential using diffraction light scattering Zeta PALS (Brookhaven Instruments, Holtsville, NY) at room temperature. Viscosity and refraction indices were set equal to those specific of water. Particle concentration was measured using a FACSCalibur flow cytometer (Becton-Dickinson, San Jose, CA). For this purpose, synthesized NPs were diluted in

water at four different concentrations. Particle concentrations were calculated using a calibration curve developed using commercially available latex particles with four different known concentrations.

2.4 Micro-architecture analysis of NP modified SIS

Lyophilized SIS was cut into 1.2 cm × 1.2 cm pieces and assembled in 1.5 ml Eppendorf tubes between the lid and the tube with mucosal side facing upwards (Figure 2-1). NPs were loaded onto the mucosal side of the SIS inserts. The inserts were incubated overnight at room temperature with constant shaking on an orbital shaker. To evaluate the micro-architecture of the NP modified SIS, the modified biomatrix was dehydrated using increasing concentrations of ethanol followed by a brief vacuum drying. Samples were then sputter coated with a 15 nm thick layer of gold at 40 mA and analyzed using a scanning electron microscope (Joel JSM-880, Stillwater, OK).

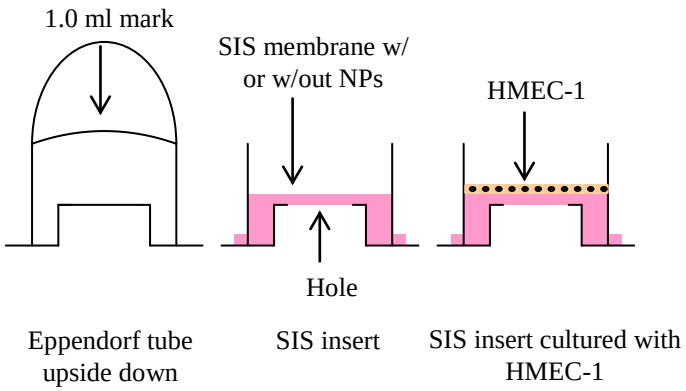

Figure 2-1 Schematic diagram of SIS inserts made from Eppendorf tubes and seeded with HMEC-1 cells

2.5 Characterization of physical Properties of PLGA NP modified SIS

SIS was made into long strips and fixed onto the inserts using silicone glue. PLGA NP suspensions with a concentration of 1.273 mg/ml were added onto the mucosal side of SIS. The assembly was placed on an orbital shaker at 37°C overnight. The NP modified SIS membranes were rinsed with water to remove unattached NPs. The thickness of the NP modified SIS was measured using our previously described method[43]. Briefly, the NP modified SIS membranes were cut into small (2 mm × 10 mm) strips. Digital micrographs of the cross section were recorded using a Nikon inverted microscope (TE300) equipped with a CCD camera. Cross section distances were measured using Sigma Scan Pro software (Systat Software Inc., Point Richmond, CA) which was calibrated using a grid image of a hemocytometer of known dimensions.

Tensile properties were also determined by our previously described method[43,144]. In brief, 6 cm × 1 cm strips of NP modified SIS membranes were cut from each sample and analyzed using an INSTRON 5842 (INSTRON Inc., Canton, MA) with a constant crosshead speed of 10 mm/min. Tests were performed under hydrated conditions at 37ºC using a custom designed chamber.

2.6 Urea permeability studies of NP modified SIS

Permeability was analyzed using the apparatus built in-house as shown in Figure 2-2. First, latex spheres or PLGA NPs were suspended in phosphate buffered saline (PBS, pH=7.4), and placed on the mucosal side of SIS in the custom-built apparatus in a way where gravity was the driving force (Figure 2-2A). NPs were allowed to settle onto the SIS on an orbital shaker at 37^{o}C overnight. The NP modified SIS membranes were washed three times with PBS in the chamber, and filled with 550 mM urea (physiological

concentration in the human urine) in PBS. PBS was then added to the serosal side of SIS in the second chamber and the apparatus was placed on its side (Figure 2-2B). Aliquots of samples (20-50 µl) were collected from the second chamber every 10 minutes for one hour and at 2 hr. The sample volumes were considered much smaller than the chamber volume (4 ml) and hence were not replaced. Samples collected immediately after the assembly of the chambers were used as time-zero values (i.e. C_2 at t = 0). Concentrations of urea were determined using a urea quantitation kit (Diagnostic Chemicals Limited, Oxford, CT).

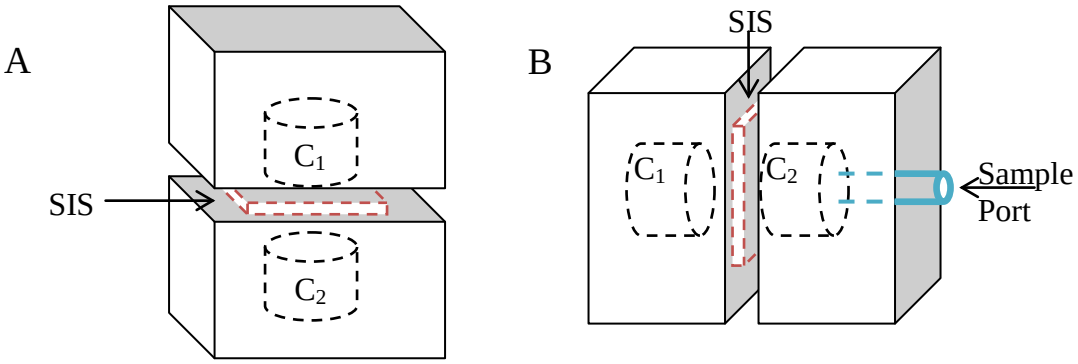

Figure 2-2 The custom-built chambers used in the study to measure urea permeability of modified SIS. A. The setup was used in this position to allow the latex spheres or PLGA NPs to go through the SIS under gravity. B. The permeability setup was used in this position to eliminate the role of gravity so that diffusion is the only driving force.

Membrane permeability was calculated as described previously[43]. In brief, Fick's first law of diffusion in one dimension defines the diffusion flux (J) as:

$$J = -D\frac{\partial C}{\partial x}$$

Where D is the diffusion coefficient (in length^2/time), C is the concentration (in amount/length^3) and x is the diffusion distance (length). Fick's second law of diffusion in one dimension states that at time t:

$$\frac{\partial C}{\partial t} = \frac{\partial J}{\partial x} \Rightarrow \frac{\partial C}{\partial t} = -D\frac{\partial^2 C}{\partial x^2}$$

In order to solve this problem, the following assumptions are made:

1. No chemical reaction takes place.
2. The diffusion is one-dimensional.
3. The diffusion is the only active force.
4. The two chambers have equal volumes at all times.
5. Quasi-steady state meaning the time it takes for the solute to diffuse through the membrane is much faster than the time it takes for the concentration to change on both sides of the membrane and hence $\frac{\partial C}{\partial t} = 0$.

This reduces the above equation to $-D\frac{\partial^2 C}{\partial x^2} = 0$. Integrating this equation and using the boundary conditions at time t=0, $C_1=C_0$ and $C_2=0$ gives the following equation:

$$\ln\left(\frac{C_0 - 2C_2}{C_0}\right) = -\left(\frac{2A_m}{V}P\right)t$$

where C_2 is the concentration of the urea measured at any time t in chamber 2, C_0 (=550 mM) is the initial concentration in chamber 1, A_m is the membrane area (=π cm^2 as the radius of the chamber is 1 cm), V is the volume of each chamber (= 4 ml), and P is the permeability of the matrix. Then $\ln\left(\frac{C_0 - 2C_2}{C_0}\right)$ was plotted as a function of time from which the slope (= $2A_mP/V$) was determined using a linear fit. The permeability was calculated using the slope values.

2.7 Evaluation of endothelial cell growth on PLGA NP modified SIS

Cultured HMEC-1 cells were used to determine whether the PLGA NP modified SIS continued to support cell growth. SIS was first assembled in Eppendorf tubes and placed in 24-well tissue culture plates as described previously[145]. PLGA NPs were placed onto the mucosal side of the SIS as described above. HMEC-1 were maintained in a complete growth medium (MCDB supplemented with 10% FBS and 1% penicillin-streptomycin) and were seeded at a density of 5.0×10^3 cells/cm^2 on the mucosal side of the SIS. To determine morphologies of HMEC-1 grown on the PLGA NP modified SIS, the cell-SIS constructs were stained with hematoxylin for 30 seconds, placed on a microscope slide, and sealed with an aqueous mounting media (Shandon, Pittsburg, PA).

Genomic DNA contents were quantitated between 3 and 7 days following cell seeding to determine numbers of cells grown on NP modified and unmodified SIS. Both modified and native SIS were taken from the same SIS batch. Briefly, cell composite SIS membranes were harvested by disassembling the SIS inserts and placing the composite in eppendorf tubes; cells were lysed with TNE buffer (10 mM Tris-HCl, pH 8.0, 150 mM NaCl, and 10 mM EDTA) supplemented with 0.2 mg/ml proteinase K (Invitrogen, Carlsbad, CA) at 55^{o}C for 2 hours according to our reported procedure[146]. Genomic DNA was subjected to phenol-chloroform extraction, ethanol precipitation, and resolved on 2% agarose gels. Images of the genomic DNA were captured by a gel documentation system (Bio-Rad, Hercules, CA). Genomic DNA band intensities were calculated using the Quantity One® image analysis software (Bio-Rad). Genomic DNA isolated from known numbers of HMEC-1 was run in parallel to construct standard curves.

2.8 Statistical analysis

Data were expressed as means ± SD. Statistical differences between two groups were evaluated using Student's *t*-test. A statistical difference was considered significant when $p<0.05$.

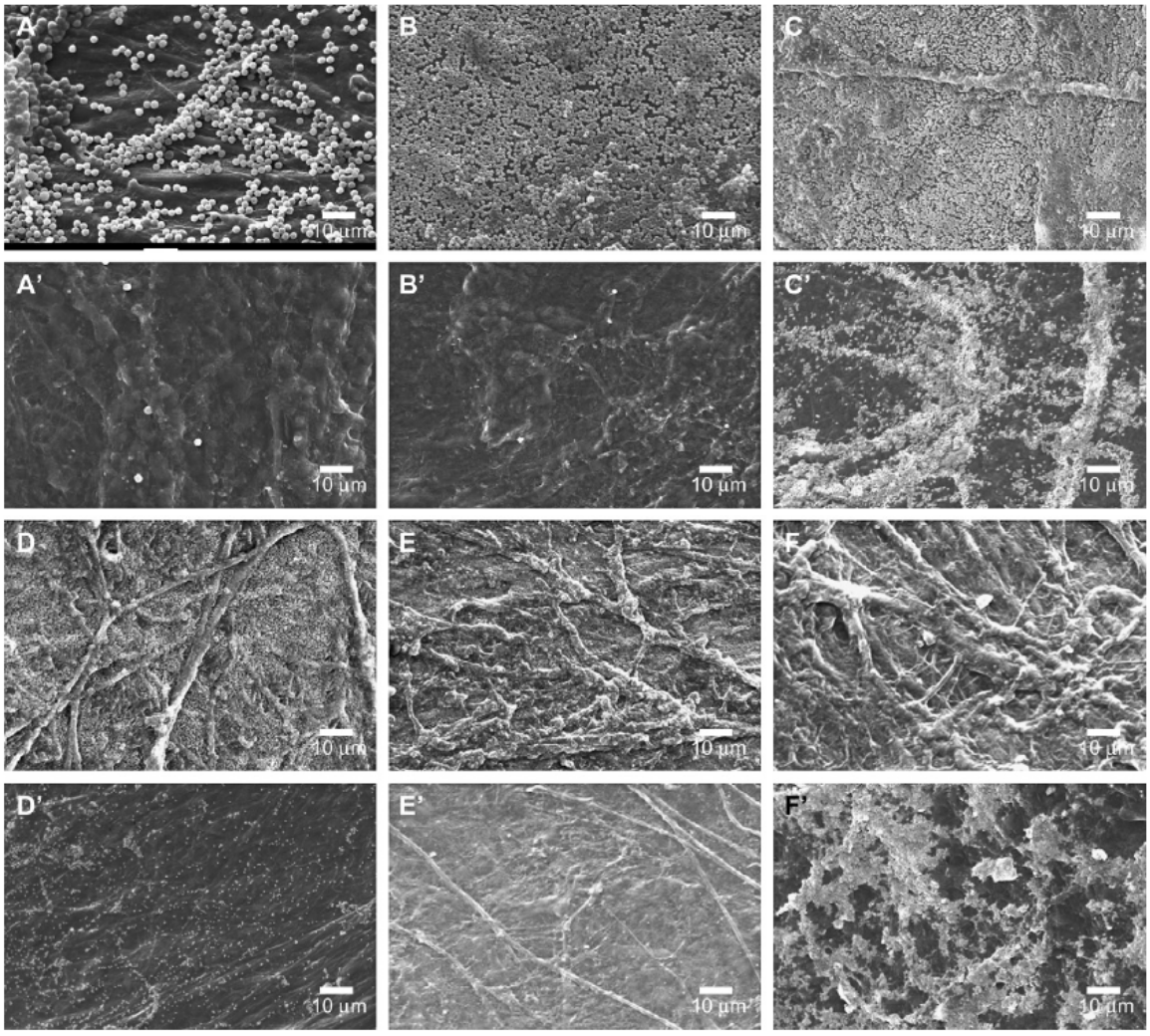

Figure 2-3 SEM images of latex spheres modified SIS. Mucosal sides of SIS were imaged following overnight embedding of A. 2 µm, B. 1 µm, C. 500 nm, D. 300 nm, E. 200 nm and F. 50 nm latex spheres. Serosal sides of the same SIS membranes were also imaged (A'-F').

3. RESULTS

3.1. Characteristics of synthesized NPs

The average diameter of synthesized PLGA NPs was 242.0 ± 9.6 nm (n=5) as determined by dynamic light scattering (DLS). Polydispersity indices varied from batch to batch, but the average value was 0.148 ± 0.036. The ζ potential (zeta potential) averaged +46.2 ± 3.4 mV. The concentration assessment by flow cytometry indicated that 1 mg PLGA NPs suspended in 1 ml water generated an average of 1.62×10^{8} particles/ml.

3.2. Surface structure of NP modified SIS

Commercial nominally monodisperse polystyrene latex spheres (sizes between 50 nm and 2 μm) were used to determine appropriate sizes of NPs to embed within SIS in order to reduce permeability to urea. Latex spheres with diameters ranging between 200 and 500 nm appeared on both mucosal and serosal sides of SIS (Figure 2-3C, C', D, D', E, E'). In contrast, larger sizes (1 μm and 2 μm) of latex spheres were predominantly present on mucosal side of SIS (Figure 2-3A, A', B & B'), whereas smaller size (50 nm) latex spheres were not observed on either side of SIS (Figure 2-3F & F'). These results suggested that NPs smaller than 200 nm could not be retained in SIS and NPs larger than 500 nm could not fit into the porous structure of SIS.

To determine whether PLGA NPs also possessed similar characteristics as latex spheres, two sizes of PLGA NPs (162 nm and 306 nm) at a concentration of 1 mg/ml were placed onto the SIS. SEM images demonstrated that both sizes of PLGA NPs (Figure 2-4) went through the SIS similar to latex spheres. However, less PLGA NPs with 162 nm in size (Figure 2-4B) were retained on the mucosal side of SIS as compared

to the serosal side (Figure 2-4B'). Furthermore, more PLGA NPs with 306 nm in size were retained on the mucosal side (Figure 2-4C) relative to serosal side (Figure 2-4C'). Nevertheless, these results confirmed that NP sizes ranging between 200-500 nm would be appropriate to fit into the porous structure of SIS.

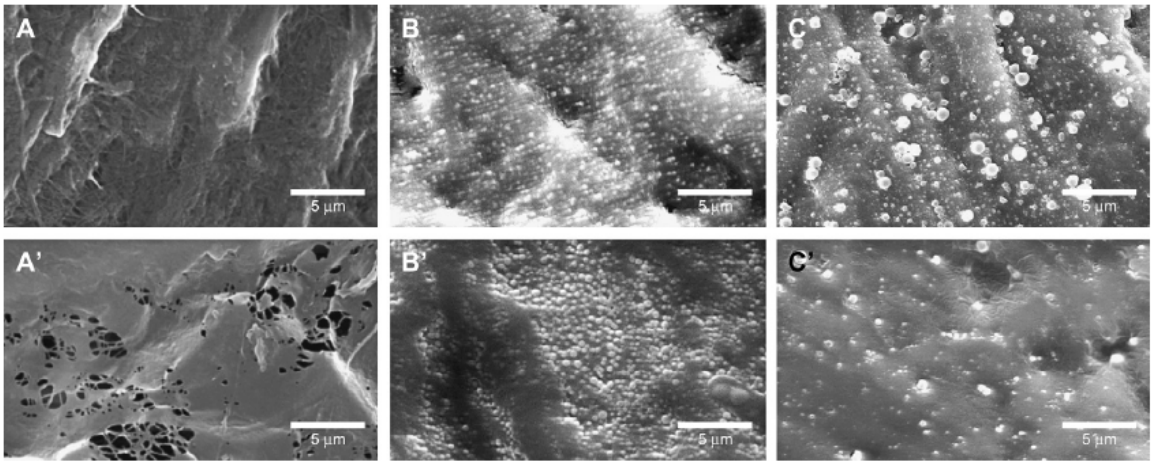

Figure 2-4 SEM images of PLGA NP modified SIS. Unmodified SIS was imaged on A. mucosal side and A'. serosal side. B. Mucosal and B'. serosal sides of SIS modified with 162 nm PLGA NPs. Panels C and C' show SIS modified by 306 nm PLGA NPs on mucosal and serosal sides of SIS respectively.

3.3. Embedded NPs altered SIS permeability

NP modified SIS had reduced permeability to urea as compared to unmodified SIS (Figure 2-5A). The permeability was 11.3×10^{-4} cm/s in unmodified SIS as compared to 7.71×10^{-4} cm/s in SIS embedded with 200 nm latex sphere. The permeability was reduced further to 6.53×10^{-4} cm/s when 300 nm latex spheres were used as compared to unmodified SIS. Both 200 nm and 500 nm latex spheres reduced urea permeability even though the reduction was not statistically significant. There was no significant difference in permeability to urea between all three sizes (200, 300 and 500 nm).

The permeability of the SIS to urea was then measured after introducing 260 nm PLGA NPs to SIS. Three different concentrations, 0.1, 1.0, and 5.0 mg/ml of PLGA NPs, were used to determine concentration dependent changes in permeability. The

permeability was significantly reduced to 5.63×10^{-4} cm/s when 1.0 mg/ml PLGA NP was used to embed SIS as compared to either 0.1 or 5.0 mg/ml PLGA NPs (Figure 2-5B).

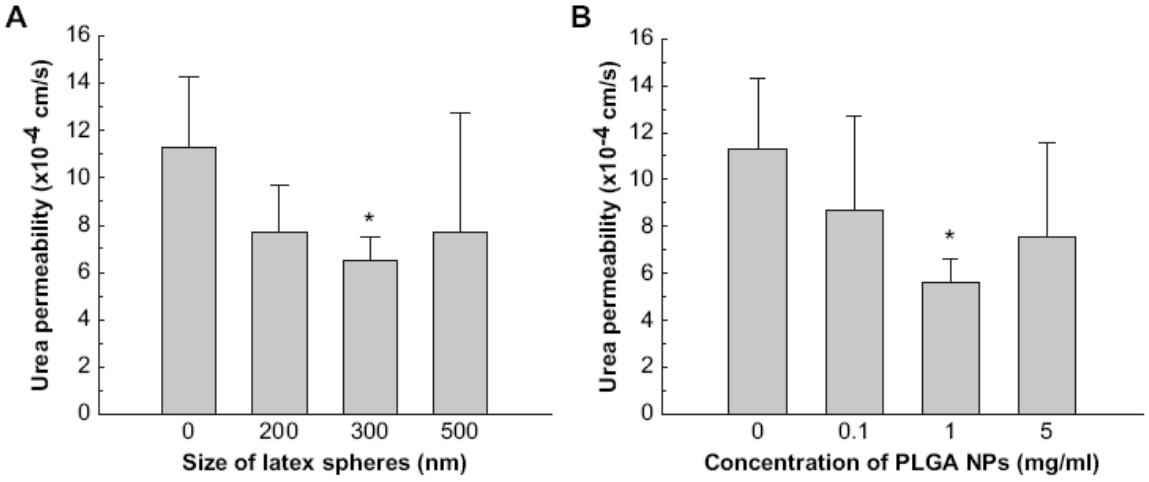

Figure 2-5 Alteration of SIS permeability to urea by NPs. Permeability chambers were set up by placing A. latex spheres or B. PLGA NPs on the mucosal side of SIS to demonstrate size-dependent and concentration dependent permeability, respectively. Zero size or zero concentration indicates permeability measured with unmodified SIS and served as a control. Results are presented as means ± SD (n=3), where * indicates $p < 0.05$ as compared to control.

3.4. NP modified SIS did not alter mechanical properties of SIS

To assess the effect of embedding NPs into SIS on mechanical property of SIS, tensile properties of PLGA NP modified and unmodified SIS were compared. These results showed no significant difference in break stress or break strain (Figure 2-6). In addition, when elastic modulus was calculated in the linear range (10 to 20% strain range), no significant difference was detected between NP modified SIS and native SIS (Table 2-1, n=12). The elastic modulus of unmodified or native SIS was about the same compared to previous reports[43]. However, the thickness of wet SIS in this study averaged 110 ± 21 μm as compared to 246 ± 16 μm in a previous report[43].

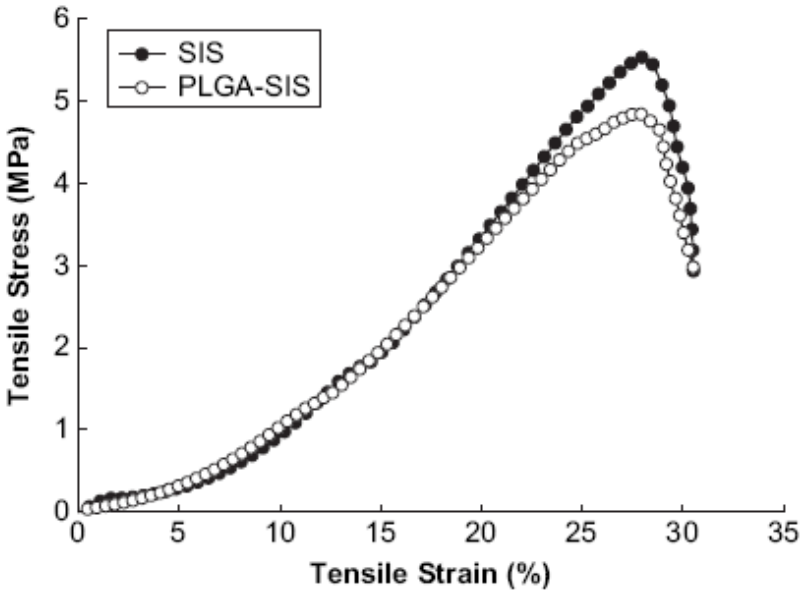

Figure 2-6 Representative sample of a stress-strain curve of native SIS and PLGA NPs modified SIS.

Table 2-1 Elastic properties of native and PLGA NPs modified SIS

Sample	Break-Point Stress (MPa)	Young's Modulus (MPa)
Native SIS	4.12 ± 0.89	21.52 ± 4.02
PLGA NPs SIS	4.24 ± 1.04	18.47 ± 4.23

3.5. NP modified SIS supported cell growth

HMEC-1 grown on both unmodified and NP modified SIS demonstrated similar morphological characteristics as shown in hematoxylin stained cell composite SIS constructs (Figure 2-7A). As expected, HMEC-1 adhered and proliferated on unmodified SIS as determined by increasing quantities of genomic DNA contents between days 3 and 7 after cell seeding (Figure 2-7B and C). Although HMEC-1 cells adhered equally well on PLGA NP modified SIS as shown by similar genomic DNA contents between NP modified and unmodified SIS on day 3. The number of HMEC-1 was 24,241 ± 3,298 on NP modified-SIS as compared to 12,336 ± 4,971 on unmodified SIS on day 7 following

cell seeding; and the difference was statistically significant ($p < 0.05$) between unmodified SIS and NP-modified SIS (Figure 2-7C).

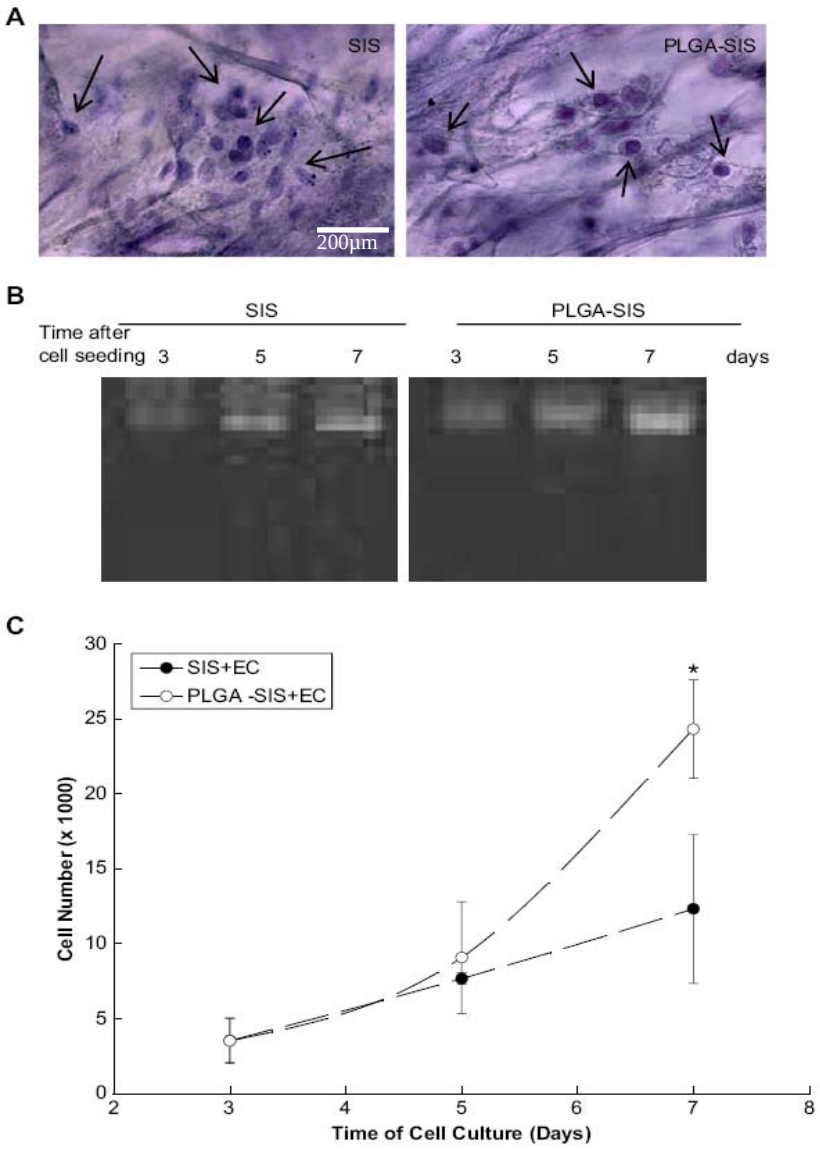

Figure 2-7 Endothelial cell growth on PLGA NP modified SIS. A. Representation of HMEC-1 cell adhesion on unmodified SIS and PLGA NP modified SIS. Arrows indicate the presence of cells in SIS structure. B. HMEC-1 proliferation on SIS as determined by genomic DNA contents was presented over a period of 7 days following cell seeding. C. Quantitation of HMEC-1 cell growth on native and modified SIS. Results are presented as means ± SD (n=4), * is where $p < 0.05$.

4. DISCUSSION

SIS has been intensively investigated for its capability in tissue repair and regeneration in a variety of tissues and animal models in the last 20 years. SIS has been shown to be a promising biomaterial for repair and regeneration in most applications due to its intrinsic ECM and growth factors[35] that may promote cell migration, growth, and differentiation. Numerous attempts have been made to produce "off-the-shelf" SIS products that would be available for clinical reconstructive surgical procedures[25,40,147,148]. However, SIS suffers from variations from batch to batch leading to different results in various applications. These inconsistencies may result from heterogeneities of this biomaterial, since mechanical properties and regenerative capability of SIS depend upon species of animals, ages of animals, and locations of small intestine being used for SIS preparation[43]. The goal of the present work was to introduce NPs to SIS in order to provide a consistent quality for this naturally derived biomaterial.

The pores in the SIS are not uniformly distributed, nor are they uniform in size[43]. This explains the wide size ranges (200-500 nm) of particles capable of embedding themselves in SIS. The absence of small size latex spheres (50 nm) within SIS in the SEM images may result from two reasons. First, 50 nm latex particles may be too small to be retained in SIS in the SEM images; or, second, the 15 nm gold used for coating during SEM procedures may make the 50 nm particles difficult or impossible to be distinguished from the SIS. It is also important to note that SIS differs from batch to batch from the same manufacturer. For example, previously we reported Cook SIS thickness as 101 ± 19.84 μm (dry) and 246 ± 16.22 μm (wet)[43]. In the present study, thickness of the Cook SIS was 29.6 ± 6.4 μm (dry) and 110 μm ± 21 μm (wet).

The permeability of SIS to urea was reduced with the embedding of the latex spheres within the SIS. That permeability to urea was reduced the most with the 300 nm latex spheres. This was evident also in the SEM images where fewer spheres were visible on the serosal side of the SIS and hence it could be inferred that more were utilized to plug the pores. Permeability studies indicated that there was no significant difference in the measured urea permeability between the 200, 300 and 500 nm latex modified SIS. This is another indication of the heterogeneity of the pore sizes of the SIS.

If we compare the SEM images for 162 nm and 306 nm PLGA NPs modified SIS in Figure 2-4, we can see more 162 nm PLGA on the serosal side of the SIS. This suggests that 306 nm PLGA NPs plugged more pores in the SIS than 162 nm NPs and thus fewer particles went through. This could also explain, why the 300 nm latex spheres reduced the permeability of the SIS to urea to a greater extent as compared to the other two sizes. It may also be possible to reduce the permeability of SIS further if a combination of different sizes of NPs is used for SIS modification.

To determine the minimal concentration of PLGA NPs that can modify SIS, 260 nm PLGA NPs were used in urea permeability assays. With 1 mg/ml PLGA NPs, the permeability was reduced significantly as compared to unmodified SIS. The failure of a higher concentration, 5 mg/ml, to significantly reduce SIS permeability to urea might result from aggregation of PLGA NPs at higher concentrations. These aggregates would form large size NPs, probably too large to fit into the porous structure of SIS, and hence could not reduce SIS permeability similar to what was seen with larger sizes of latex spheres (1 and 2 μm).

The observation that PLGA NPs remained attached to or embedded within the SIS is very important especially if they will be used for delivery of therapeutics. It could take up to 16 weeks before the SIS is completely resorbed[43] while the PLGA NPs (200 nm) will degrade in no more than 2 months[65]. This feature allows the NPs to remain attached to the SIS and deliver their load before the biomaterial is completely dissolved.

Reduction in SIS permeability may be a critical factor in determining the success of tissue repair and regeneration especially in bladder regeneration. Based on previous observation, proximal sections of SIS, that are more permeable to urea than distal sections of SIS[43], have not been successful for bladder regeneration[42]. The leakage of urine in augmented bladder can have detrimental effects on inflammatory responses during the process toward complete regeneration, and may result in the absence of bladder regeneration as we reported in a dog bladder augmentation model[42]. We expect that the reduction in permeability in NP modified SIS will significantly improve tissue regeneration processes particularly in urinary bladder regeneration.

The mechanical properties of the SIS stayed the same after modification with PLGA NPs. The reason the elasticity did not change in the modified SIS compared to native is that the elasticity is an inherent property of the collagen fibers within the SIS. Since the NPs were not embedded within the collagen fibers, we did not expect the elasticity to change. This is very important because we sought to change only the physical properties of the SIS and not the mechanical properties. Changing the mechanical properties might interfere with the cell-biomaterial interactions as well as with the compliance of the biomaterial, which might in turn effect the compliance of the tissue it is intended to replace or regenerate, especially the bladder tissue.

The most significant observation was that PLGA NP modified SIS continued to support cell adhesion and growth. Since SIS interferes with various assay systems including colometric-based, fluorescence-based, and ^{3}H-thymidine incorporation assays for determining cell proliferation, these assays are not appropriate for quantitating *in vitro* cell growth on SIS. In this study, the number of cells growing on SIS were estimated by quantitating the amounts of extractible genomic DNA. PLGA NP modified SIS did not interfere with HMEC-1 growth as demonstrated by the similar quantity of genomic DNA extracted from both unmodified and modified SIS on day 3. In addition, it is important to note that without cell adhesion there could be no growth. Therefore, even though a separate experiment was not conducted to test the effect of the modified SIS on cell adhesion, it is likely that PLGA NPs did not interfere with HMEC-1 adhesion to the SIS.

HMEC-1 grew gradually on unmodified SIS between days 3 and 7 as we expected. Interestingly, HMEC-1 proliferation was significantly higher on PLGA NP modified SIS as compared to unmodified SIS on day 7. The mechanism that is responsible for the enhanced cell proliferation in PLGA NP modified SIS is not clear. The elevated cell proliferation might result from a uniform porous structure provided by NP modified SIS for easier cell migration and distribution, or synergistic effects of PLGA and SIS to support and enhance cell growth[10,149,150].

The continued growth of HMEC-1 cells on the modified SIS eliminates any concern about the effects of the degradation products of the PLGA NPs: lactic acid and glycolic acid on cellular functions. One major concern of using PLGA NPs in tissue engineering is that these products might alter the microenvironments and interfere with cell physiology in a negative fashion. However, our experiments have indicated otherwise.

In conclusion, PLGA NPs within a size range of 200-500 nm reduced the permeability of SIS to urea without interfering with the material's mechanical properties. The PLGA modified SIS continued to support HMEC-1 growth, which was significantly enhanced by day 7 of cell culture, compared to native SIS.

Future studies could address the possibility that a combination of different sizes of NPs could ultimately be needed to achieve maximal uniformity of SIS based on the variations of the SIS pore size as well as of the material from batch to batch.

Another avenue that this study focused on was the use of PLGA NPs to deliver hyaluronic acid at the same time of being used to modify the SIS. The rationale for using hyaluronic acid was provided in Chapter 4. However, if the delivery of exogenous HA would be feasible, expression of HA and HA receptors in regenerated tissue need to be determined because HA works by binding to and activating its receptors. Delivery of HA to tissue may prove useless if there are no HA receptors in that tissue. The studies to determine the expression of HA and HA receptors in regenerating rat bladder were described in Chapter 3.

Chapter 3 Temporal Expression of Hyaluronic Acid and Hyaluronic Acid Receptors, CD44 and LYVE-1, in a Rat Bladder Regeneration Model Using Porcine Small Intestine Submucosa Scaffold

1. INTRODUCTION

Tissue engineering technology is intended to restore or replace aplastic, hypoplastic, or pathologic tissues or organs. Reconstruction or replacement of abnormal bladder to restore bladder function is one of the most intensely studied applications in the field of tissue engineering. Currently, two methods of bladder tissue engineering exist. The seeded technique involves harvesting host tissues to extract bladder cells (urothelial and smooth muscle) and culturing them to increase densities. These cells are then seeded onto a biodegradable acellular matrix *ex vivo* and implanted into the host organ for continued regeneration processes[11]. An alternative to the seeded technology is the unseeded technique. This technique involves implanting an acellular matrix, without prior cell seeding, directly into the host organ and allowing the host cells to repopulate the matrix and regenerate the tissue[40]. Both of these techniques have been shown to produce normal bladder tissue based on histological and functional criteria[11,28,151].

Hyaluronic acid (HA) is a non-sulfated glycosaminoglycan and an integral part of the extracellular matrix (ECM) widely distributed in connective, epithelial and neural tissues. It is a normal constituent of the basement membrane. HA is composed of alternating (1 $\rightarrow$ 4)-β linked glucouronic acid and (1 $\rightarrow$ 3)-β linked N-acetyl-$_D$-glucosamine. HA mediates a wide range of cellular activities including cell migration, cell-cell and cell-ECM adhesion, cell differentiation, cell proliferation, morphogenesis, inflammation as

well as angiogenesis[113]. HA has been studied in wound healing and tissue regeneration[111,120]. HA is believed to be actively involved in repair and regeneration processes based on its unique viscoelastic and rheological properties through binding to its receptors[118]. There are five HA receptors being identified currently, including CD44, LYVE-1, HARE, VEGFR-3 and RHAMM.

In urinary bladder regeneration, HA has been incorporated into bioscaffolds to improve the outcomes of the regeneration process[152,153]. HA works by binding and activating its receptors. However, there is no report showing temporal and spatial distribution of HA and its receptors in regenerative bladder tissue.

Small intestinal submucosa (SIS) harvested from porcine small intestine has the capability of promoting urinary bladder regeneration without cell seeding[28,42]. Recent reports indicate that SIS derived from distal sections (300-400 cm proximal to the ileocecal valve) of porcine small intestine can promote complete regeneration in rodent[154]and canine bladder regeneration models[42]. This study was conducted to determine the temporal and spatial expression of HA and HA receptors in a SIS augmented rat urinary bladder regeneration model to determine if it would be physiologically relevant to deliver exogenous HA to the SIS.

2. MATERIALS AND METHODS

2.1 Reagents

Peracetic acid, bovine serum albumin (BSA) and biotinylated hyaluronic acid binding protein (HABP) were obtained from Sigma-Aldrich Inc. (St. Louis, MO). Mouse anti-rat CD44 monoclonal antibody and rabbit anti-human polyclonal antibody VEGFR-3 were obtained from Chemicon International (Temecula, CA). Rabbit anti-human LYVE-1

polyclonal antibody was obtained from Abcam (Cambridge, MA). Goat anti-human RHAMM polyclonal antibody was obtained from Santa Cruz (Santa Cruz, CA). Mouse anti-rat HARE monoclonal antibody was obtained from Dr. Paul Weigel (Department of Biochemistry and Molecular Biology, OUHSC). Goat serum and stable DAB (diaminobenzidine) were obtained from Invitrogen Inc. (Carlsbad, CA). Fast red substrate was purchased from BioGenex (San Ramon, CA). Streptavidin-conjugated horseradish peroxidase (HRP) was obtained from Vector Laboratories Inc. (Burlingame, CA). Streptavidin-conjugated alkaline phosphatase (AP) was obtained from BioLegend (San Diego, CA). Hematoxylin was obtained from Anapath Inc (Lewisville, TX).

2.2 Animals

Eighteen Sprague-Dawley adult female rats weighing 275-300 g were obtained from Charles River Laboratories (Raleigh, NC). Three rats were used as surgical controls. The experimental animals were housed in the university animal care facility with free access to food, water and standard light/dark cycles. Procedures used in this study have been approved by the Institutional Animal Care and Use Committee (IACUC).

2.3 Preparation of SIS

SIS was prepared from the distal segment of porcine ileum obtained from a 3-year old sow (from a slaughter facility, Weatherford, OK) as previously described[154]. Briefly, the tunica mucosa and the serosa muscularis were mechanically removed. All segments with Peyer's patches were discarded. SIS membranes were sterilized by exposing them to 0.1% peracetic acid for 1 hour followed by three washes with sterile distilled water for 5 minutes each. The SIS was then stored in sterile water at 4^{o}C for up to six months. No

digestive enzymes or solutions were used in the production of the SIS biomaterial. All experiments were performed using the same batch of SIS.

2.4 Surgical procedures for bladder augmentation

Rat bladder augmentation was performed using our previous reported procedure[155]. Briefly, rats were anesthetized by intraperitoneal injection of ketamine (100 mg/kg). Abdominal hair was clipped and the skin was prepped for sterile surgery. A 3 cm midline abdominal incision was made and continued down to the peritoneal cavity. An approximate 1 cm^2 square area of the bladder dome was removed; and replaced with a similar sized SIS sutured to the native bladder margin using 6-0 Vicryl (Ethicon, Somerville, NJ) in a watertight fashion. Permanent 6-0 Ethicon marking suture was used to determine the graft area. The abdominal wall was then closed. The animals were then returned to normal housing. Three rats that did not have any surgical manipulation were used as unaltered controls.

2.5 Tissue processing

Rats were euthanized with lethal doses of pentobarbital on post-operative days 2, 7, 14, 28, and 56. There were three rats in each time group and three control rat bladders. The bladders were harvested, inflated with 10% formalin and fixed in 10% formalin for 24 hours. The bladders were then divided by a midline longitudinal incision and embedded in paraffin. Paraffin sections were cut at 5 μm and mounted on glass slides, incubated at 65°C for 30 minutes, and stored at room temperature until immunohistochemical staining was performed.

2.6 Immunohistochemical analysis

Hematoxylin-eosin (H & E) staining was performed with an automatic slide stainer (Tissue-Tek DRS 2000; Sakura, Torrance, CA). For immunohistochemistry, the bladder sections were dewaxed in xylene, rehydrated in a series of graded alcohol, then in distilled water followed by rinses with 0.01M Tris-buffered saline (TBS) as previously described[156]. Endogenous peroxidase activity was eliminated with the application of 1.6% hydrogen peroxide in TBS for 30 minutes. Tissue sections were incubated with TBS containing 10% goat serum and 1% bovine serum albumin (BSA) for 2 hours at room temperature to block non-specific binding. To detect HA receptors' expression, slides were then incubated with 1:400 mouse anti-rat CD44 antibody, 1:1200 rabbit anti-human VEGFR-3 antibody, 1:800 rabbit anti-human LYVE-1 antibody, 1:400 goat anti-human RHAMM antibody, or 1:2000 mouse anti-rat HARE antibody in TBS supplemented with 1% BSA. A separate slide was incubated with the diluent without primary antibody and used as a negative control. Following rinses with TBS, the tissue sections were incubated with biotinylated goat anti-rabbit (VEGFR-3 and LYVE-1), biotinylated horse anti-mouse (CD44 and HARE), or biotinylated rabbit anti-goat (RHAMM) secondary antibody diluted to 1:400 with TBS with 1% BSA and incubated at room temperature for 2 hours. Following rinses with TBS, streptavidin-HRP (horseradish peroxidase) diluted to 1:400 with TBS and 1% BSA was added and incubated for 30 minutes at room temperature followed by another rinse with TBS. The bound antibodies were visualized by incubating the slides with stable 3,3'-diaminobenzidine (DAB) for four minutes. The color development was terminated by washing the slides with tap water. The slides were then lightly counterstained with hematoxylin for 20 sec, rinsed in

tap water, dehydrated in graded alcohol, cleared in xylene, mounted with mounting medium, and cover slipped.

For HA staining, slides were incubated with 1:200 1mg/ml biotinylated HABP for 2 hours after blocking with 10% goat serum with 1% BSA. Following rinses with TBS, the tissue sections were incubated with 1:400 streptavidin-HRP and incubated at room temperature for 2 hours. HABP binding was visualized by incubating the slides with fast red for 20 minutes at room temperature. After washing with tap water, the slides were counterstained with hematoxylin for 20 sec, rinsed in tap water and mounted with aqueous mounting media. Microscopic images were taken with a Nikon Eclipse 80i (Nikon, Japan) microscope.

2.7 Quantification of LYVE-1 positive lymphatic vessels

Lymph vessels that stained positive for LYVE-1 in the augmented and native bladders were counted blindly. The results were reported as average ± standard deviation of 3 animals in each time point.

2.8 Statistical analysis

Data were expressed as means ± SD. Statistical differences between two groups were evaluated using Student's *t*-test. A statistical difference was considered significant when $p<0.05$.

3. RESULTS

3.1. Inspection of bladder tissue regeneration

Histological presentations of regenerated bladder were inspected by H & E staining of bladder tissues. Similar to prior studies, the SIS augmented bladder regeneration proceeded without complications[154]. Complete urothelium covering the entire SIS graft

with hyperplastic changes and folding was evident by day 14 of the regeneration process (Figure 3-1). By day 28, the urothelium layer (URO) was thinner and early fibroblasts were identified. A mature urothelium and smooth muscle layer was visualized at day 56 as previously reported[154].

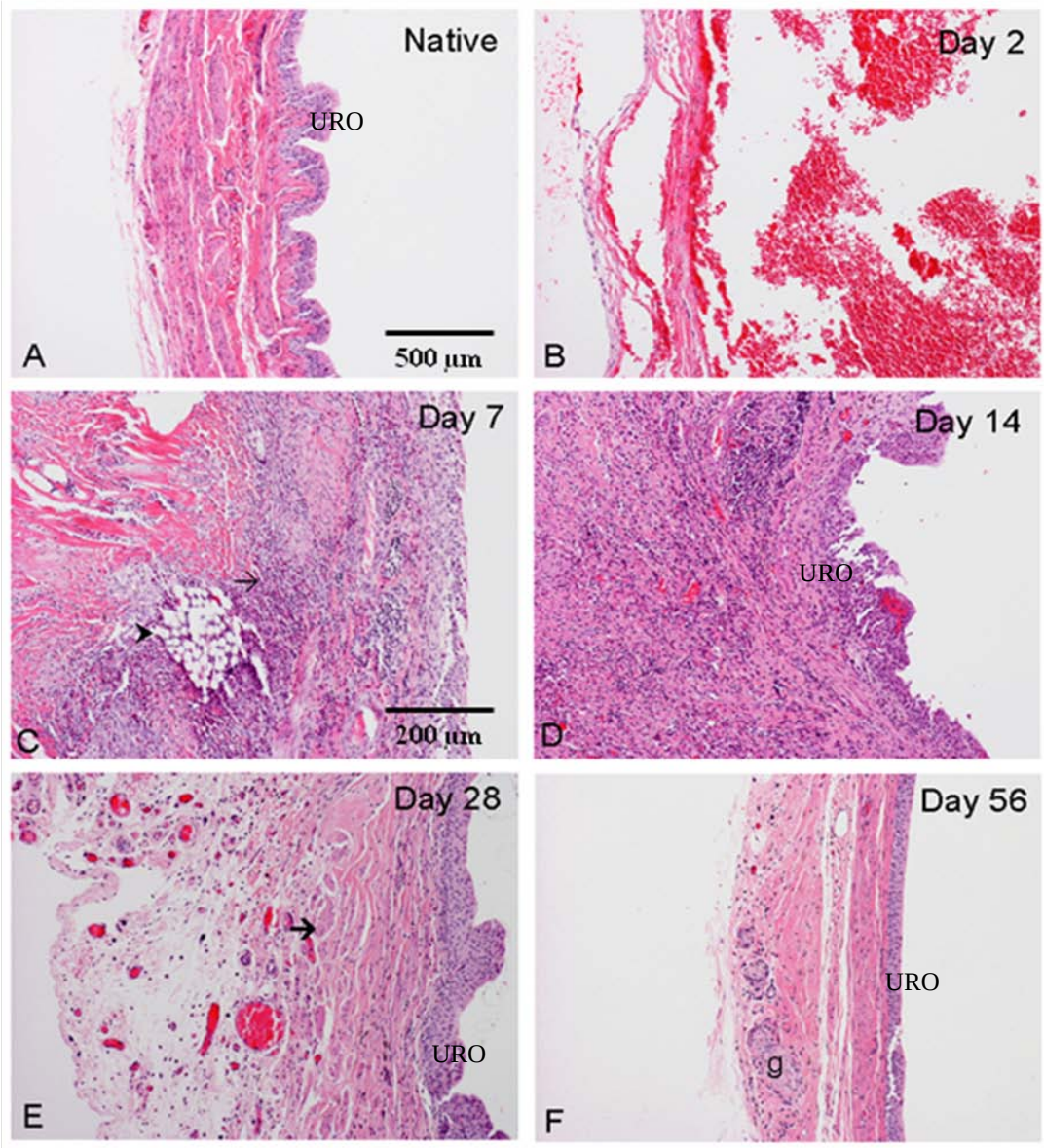

Figure 3-1 H & E staining of SIS-augmented rat bladders. A. Native bladder for comparison. B-F. The graft portion of the augmented bladders. These augmented bladders were harvested on days 2, 7, 14, 28 and 56 post-operation. The suture materials (arrowhead) are identified and confirmed the site of operation. Urothelial (URO) covering is almost complete by day 14. There is inflammatory cell infiltration in response to the surgery (small blue cells identified by the thin arrow) but inflammation is largely resolved by day 28. Regenerating smooth muscle fibers can also be identified in the regenerating site (thick arrow). Note the giant cell granuloma in response to the suture material located in the graft site (g). Original Magnification: 10× in B-E and 4× in A and F.

3.2. Temporal deposition and spatial distribution of HA

The presence of HA in bladder tissues was detected by HABP through its specific binding to HA. There was no detectible HABP binding in control normal bladder. In the native and regenerating sections of the SIS augmented bladders, there was no HA binding activity up to 14 days post-operation. In contrast, a strong HABP binding activity was observed in both the augmented and native portions of the regenerating bladders at days 28 and 56 post-operation. The HA reactivity was mainly localized to the ECM of the connective tissues (Figure 3-2).

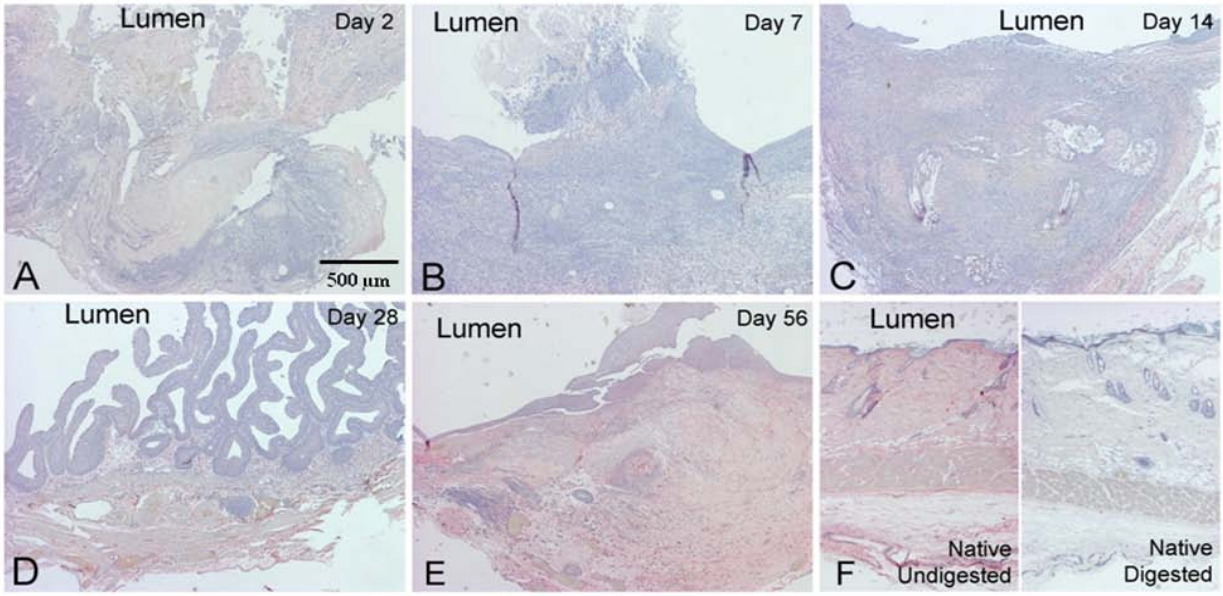

Figure 3-2 Immunohistochemical staining for HA in the graft portion of the SIS-augmented rat bladders. A-E. HA immunoreactivity was determined on days 2-56 post-augmentation in SIS graft sections of regenerating bladders. The lumen of the bladder is indicated. F. Rat skin was stained in parallel and used as a positive control and tissue section digested with hyalurodinase was included as a negative control. The expression of HA in ECM is evident in red. Original magnification: 4× in all panels.

3.3. Temporal expression and spatial distribution of HA receptors

CD44

CD44 immunoreactivity in the regenerating bladders was minimal between day 2 and 14 post-augmentation. On day 28 post-operation, the CD44 immunoreactivity appeared to

have increased. By day 56 post-operation, a strong CD44 immunoreactive signal was detected in bladder urothelial cells as well as in lymphocytes in the both the native and augmented portions of the regenerated bladders (Figure 3-3).

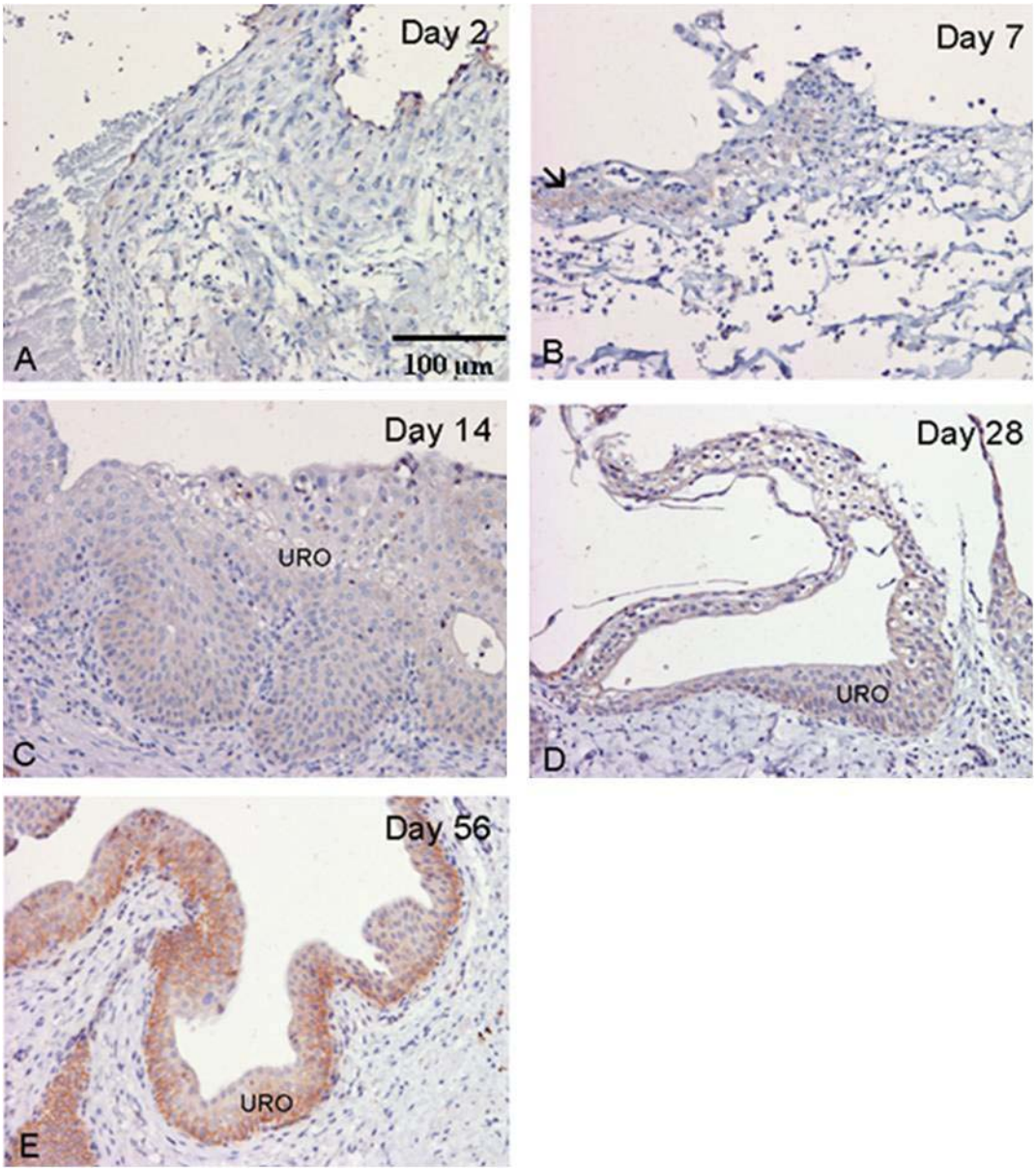

Figure 3-3 Immunohistochemical staining for CD44 in the graft portion of the SIS-augmented rat bladders. A-E. CD44 immunoreactivity was determined on days 2-56 post-augmentation. CD 44 immunoreactivity is mainly located in urothelium, and staining intensity increased as urothelial cells differentiated. In day 7 (B), only a small amount of regenerating urothelium is present (arrow). A gradual increase in the immunoreactivity for CD44 is noted in the urothelium (URO) from day 14 to 56 (C-F). Original magnification: 20× in all panels.

LYVE-I

LYVE-1 immunoreactivity was not detected until day 28 (D28) and day 56 (D56) post-augmentation (Figures 3-4A & B). The lymph vessels showed strong LYVE-1 immunoreactivity in both the augmented and native sections of the bladders. There was also strong expression of LYVE-1 in the native bladder (Figure 3-4C). Quantitative analysis of LYVE-1 positive lymphatic vessels (n=3) showed that the augmented bladders at days 28 and 56 post-operation revealed 2.78 ± 1.56 lymph vessels /mm^2 and 1.95 ± 1.23 lymph vessels /mm^2, respectively (Figure 3-4D & Table 3-1). The native control bladder had 3.44 ± 0.06 lymph vessels /mm^2. There was no expression of LYVE-1 at the earlier time points, days 2, 7 and 14 (D2-D14). There was no statistical difference in number of lymphatic vessels between normal and augmented bladders according to Student's t-test.

VEGFR-3, RHAMM and HARE

HARE immunoreactivity was weak and sometimes not evident in both native and augmented bladder tissues at all time points. Commercially available primary antibodies against RHAMM and VEGFR-3 failed to demonstrate proper staining in rat bladder sections.

Table 3-1 Quantification of lymph vessels in native and augmented rat bladder

Sample	**Lymph vessels/mm^2 (±SD)**
D28 SIS	2.78 ± 1.56
D56 SIS	1.95 ± 1.23
Native SIS	3.44 ± 0.06

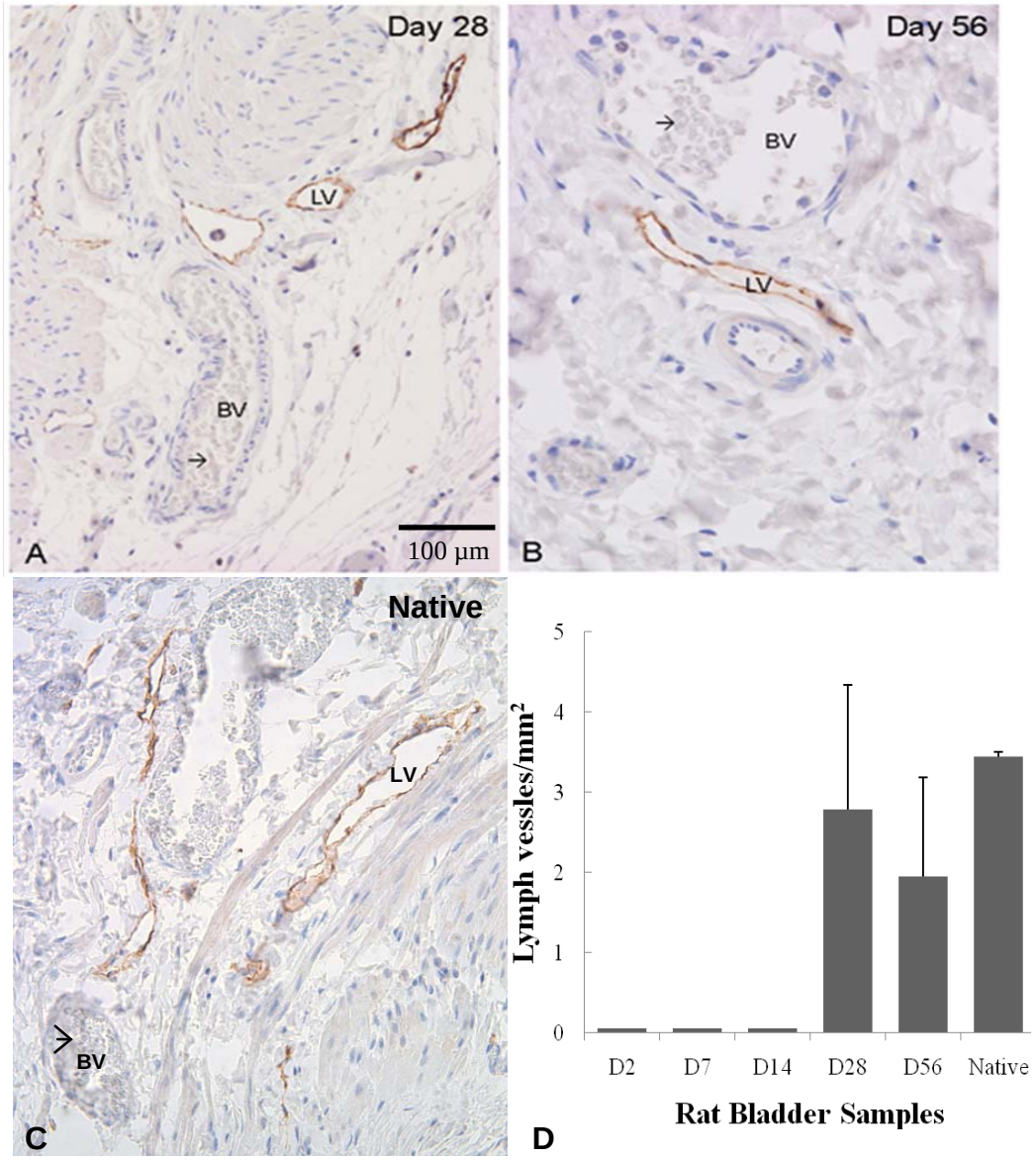

Figure 3-4 LYVE-1 immunoreactivity in SIS-augmented rat bladder. Immunohistochemical staining of regenerating bladder on A. day 28 and B. day 56 post-augmentation. C. Expression of LYVE-1 in native bladder is presented as a control. The expression of LYVE-1 in the lymph vessels is evident. The endothelial cells of lymphatic vessels (LV) are immunoreactive but the endothelial cells of blood vessels (BV) are non-reactive. The red blood cells are indicated by the arrow. D. Lymph vessel counting was performed for all samples (n=3). There was no expression of LYVE-1 at earlier time points (D2-D14). Original magnification: 40× in all panels.

4. DISCUSSION

HA plays an important role in cell migration, proliferation, differentiation, morphogenesis, inflammation, and angiogenesis[113]. Based on these biological properties,

HA is considered an important component for promoting wound healing and has been incorporated into bioscaffolds to improve the outcomes of tissue regeneration[152,153]. However, there is no data demonstrating whether HA is deposited in regenerating tissues endogenously or whether HA receptors are expressed at any phase of the regeneration process. This study represents the first characterization of HA and its receptors in a rat bladder regeneration model.

We followed the expression of HA, as well as of CD44 and LYVE-1 during the process of wound healing and regeneration during the course of bladder regeneration. HA localization and HA receptor expression followed the same temporal pattern during the regeneration process. As determined by immunoreactivity produced by HABP, HA is detected specifically in the ECM of both native and augmented portions of the regenerating bladder after 28 days post-operation, but not in control bladder. This result is consistent with reports from skin wound healing[157] and cancer development[158] where results show an abundance of HA in the ECM. In addition, Dechert et al. showed that a decline in the levels of HA occurred on the days that the inflammation was the highest, suggesting that HA levels in chronic wounds could be affected by inflammation[159]. The rat bladder augmentation model could be considered similar to a chronic wound model as inflammation persists on the early time points (days 2-14) and recedes on the later time points (days 28 and 56). This could explain the absence of HA in augmented rat bladder during the early phases of wound healing between days 2 and 14 and its presence on days 28 and 56. However, there are clearly elevated levels of HA in regenerating tissue at 56 days post-augmentation when the healing process has completed as indicated by the H&E staining. These results show the complexity of the parameters that control HA synthesis

and suggest that delivery of exogenous HA to chronic wounds may be preferred at later time points when inflammation have receded and more HA receptors are available.

Although it would be highly informative to quantify the amount of HA present during the regeneration process, this was not feasible in the present study. One way to quantify HA in tissue is using western blot and an antibody specific to HA such as HA binding protein (HABP). However, the problem with this is when running gel electrophoresis, where the HA shows as a smear of bands instead of the typical one distinct band characteristic of proteins. This is because the common way of preparing HA of desired sizes is through digestion with hyalurodinase. This enzyme creates fragments of HA of multiple sizes. The desired size is simply the average, hence the smear of multiple bands in the gel. Another alternative way to quantitate HA is by using high performance liquid chromatography (HPLC). Unfortunately, we did not have access to such machinery.

CD44 is a major receptor for HA. CD44 is widely expressed in epithelial, mesenchymal, and lymphoid cells in nearly all tissues[142]. CD44 has been shown to be involved in angiogenesis as CD44 knockout mice showed inhibition of vascularization in matrigel implants[160]. In this study, CD44 was mainly expressed in urothelial cells by day 56 post-operation, which coincided with urothelial cell differentiation as previously reported[154]. Could there be a connection between CD44 and epithelial differentiation? Indeed there is, as Witt and Kasper showed in the development of taste buds that CD44 expression appeared in the marginal epithelium cell membrane of early taste buds, and by late gestation and perinatally that expression has completely shifted to intragemmal cells, suggesting a role of CD44 in the differentiation of the taste bud cells[161]. Yamazaki et al. also showed that CD44 expression on the apical surface of osteoclasts and chondroclasts

did not occur strongly until day 21 of the fractured callus when the fracture was almost completely remodeled[162].

It is possible that accumulation of HA could be responsible for overexpression of CD44. At this point, we cannot determine the order in which HA or CD44 are expressed. Also, modulation of the HA-cell interaction during chondrogenic condensation in the embryonic chick limb parallels the expression initiation of CD44[163]. These findings demonstrated similar temporal appearance of HA and its major receptor, CD44, at day 28 post-augmentation in this study.

LYVE-1, cell surface HA receptor, shares similar structure with CD44 with different functionality[142]. LYVE-1 is expressed almost exclusively in endothelial cells of lymphatic vessels but not endothelial cells of blood vessels[142]. Consistently, we observed that LYVE-1 was exclusively localized to lymph vessel endothelium only in regenerating bladders. Similar to the targeted expression of CD44 and HA, LYVE-1 was not detected in regenerated rat bladder until day 28 post-operation. The expression of LYVE-1 was strong both in the native and augmented parts of the bladder. We have previously shown that the inflammatory response in rat bladder augmented with SIS is most pronounced during the first two weeks of tissue regeneration[155]. By day 28, most of the inflammation has receded. Expression of LYVE-1 can be regulated by inflammatory regulators[164]. Johnson et al. showed that incubation of pro-inflammatory cytokine tumor necrosis factor (TNF) with primary human dermal lymphatic endothelial cells (HDLEC) resulted in complete loss of LYVE-1 expression[164]. This may explain why LYVE-1 in lymph vessels was absent until day 28 when the inflammatory response was reduced. A similar explanation to the temporal co-expression of HA-CD44 might be applicable here. It is

very possible that accumulation of HA could be responsible for over expression of LYVE-1. At this point, it is not quite clear what is the mechanism behind the expression of these receptors.

The goal of the present study was to determine temporal and spatial expression of HA in a regenerated tissue. Having HA receptors in the regenerated tissue is an important requirement for delivery of exogenous HA, which might prove useless if the receptors are not available. However, it was not clear from the IHC staining of LYVE-1 alone if any differences existed in the expression between days 28 and 56 post-augmentation. On the other hand, from the staining for HA and CD44, there was clearly more HA and CD immunoreactivity on day 56 post-augmentation.

In conclusion, HA localization and expression of its receptors, CD44 and LYVE-1, show similar pattern of expression becoming evident at day 28 post-augmentation in rat bladder model. Delivery of exogenous HA to regenerated tissue is therefore a realistic avenue because of the presence of receptors that can bind and interact with HA. As discussed earlier, HA receptors were not present until day 28 post-augmentation. Therefore, delivery of exogenous HA could be established at later time points of the regeneration process when the proper receptors are available and inflammation has receded. However, we should not rule out the possibility that exogenous HA could be delivered at earlier time points. We do not know if elevated levels of HA could cause over expression of HA receptors although it is very possible. Based on his possibility, the delivery of HA to regenerated bladder could begin at the earlier time points of regeneration and continue until the regeneration process is complete, as discussed above.

In Chapter 2 we have shown that PLGANPs modified SIS can improve endothelial cell growth while yielding more consistent outcome for regeneration. Therefore, the following studies, examining the delivery of HA to the SIS using PLGA NPs were described in the next chapter.

Chapter 4 Enhanced angiogenic potential of porcine small intestine submucosa via hyaluronic acid-poly(lactide-co-glycolide) nanoparticles: From fabrication to pre-clinical validation

1. Introduction

Nanotechnology involves the formulation and manipulation of materials to create unique products with novel properties at the nanoscale level. PLGA NPs are submicron-sized colloids designed to deliver biologic molecules of interest either encapsulated within or condensed/conjugated on the surface of the particles[44]. In this study, we explore the use of HA-PLGA treated biocompatible material (SIS) in tissue regeneration without cell seeding.

HA is a major component of the extracellular matrix (ECM) and has been intensely studied for its roles in tissue development, wound healing, regeneration, tumor invasion and cell-cell interactions[122,165,166]. HA-modified bioscaffolds have been investigated in the field of regenerative medicine to improve angiogenesis and tissue regeneration[83,167].

Identification of a biocompatible material is the first critical step in scaffold-induced tissue regeneration. SIS has been investigated as a bioscaffold to repair and replace a variety of tissues. Unlike synthetic biomaterials, SIS supports cell ingrowth, differentiation, and tissue regeneration without prior cell seeding[42]. However, the use of SIS in tissue engineering has been limited because of its inconsistency in supporting tissue regeneration for large areas[168] and its location-dependency[43]. This deficiency is common in naturally derived biomaterials and likely contributes to the contradicting results obtained by using these materials. Our prior work (Chapter 2) demonstrated that

physical and biological properties of SIS could be modified using PLGA NPs while maintaining the structural integrity of the biomaterial. We also showed (Chapter 3) that HA and its receptors, CD44 and LYVE-1, are present in regenerating rat bladder. In this study, we sought to deliver HA using these PLGA NPs and study the effect of HA-PLGA NPs on endothelial cell growth and the angiogenic potential of the SIS modified with HA-PLGA NPs in *in vitro* CAM model and *in vivo* dog model.

2. Materials and methods

2.1. Reagents

PLGA was purchased from Absorbable Polymers International (Pelham, AL) as a 50:50 monomer ratio with molecular weight of 106 kDa and viscosity of 1.05 dL/g. Hyaluronic acid with an average molecular weight of 74 kDa was purchased from Life core Biomedical (Chaska, MN). Single layer SIS (Surgisis®) was provided by Cook® Biotech (West Lafayette, IN). Human mammary endothelial cells (HMEC-1) were provided by Dr. Mike Ihnat at the University of Oklahoma Health Sciences Center[143]. Fertile leghorn chicken eggs were purchased from CBT Farms (Chestertown, MD).

2.2. Animals

Fifteen adult male beagle dogs with an average weight of 14 kg were obtained from Ridglan Farms (Mt. Horeb, WI). These animals were housed in the university animal care facility with free access to food, water and standard light/dark cycles. All procedures for animal studies were in compliance with the Institutional Animal Care and Use Committee (IACUC) approved protocol.

2.3. Synthesis of HA-PLGA NPs

PLGA NPs were synthesized using a double emulsion technique[169] that was modified with polyethylene imine (PEI) to produce cationic NPs. Briefly, 30 mg of PLGA was first dissolved in 1 ml of chloroform. An aliquot of 200 µl of 7% PEI was added to the PLGA/chloroform solution followed by sonication on ice with a probe sonicator for 30 seconds. The primary emulsion was transferred into 10 ml of 1% PVA; and the entire solution was sonicated on ice for another 1 min. The organic solvent in the final solution was allowed to evaporate overnight with continuous stirring. PLGA NPs were recovered by centrifugation at 30,000 × *g* for 20 min at 4^{o}C. The pellet was resuspended in water and freeze-dried for two days. A known amount of lyophilized PLGA NPs was resuspended in PBS pH 7.4 to get a 1 mg/ml stock solution. Different amounts of HA were mixed with a constant weight of 100 µg PLGA NPs to produce pre-determined w:w ratios and incubated at room temperature for 10 minutes. The HA-PLGA NPs were then centrifuged at 20,000 ×g at 4^{o}C for 20 min. The pellet was resuspended in PBS (pH 7.4) and centrifuged at 20,000 ×g at 4^{o}C for 20 min three times to remove any unbound HA. The multiple washes were saved for later assay of HA. HA-PLGA NPs were finally resuspended in PBS (pH 7.4). The HA-PLGA NPs were prepared fresh for every experiment.

2.4. Characterization of HA-PLGA NPs

The size, polydispersity index, and zeta potential measurements of synthesized HA-PLGA NPs were determined using diffraction light scattering Zeta PALS (Brookhaven Instruments, Holtsville, NY). Viscosity and refraction indices were set equal to those specific of water. Surface morphology of the NPs was examined using a JOEL-JSM-880

scanning electron microscope (SEM). Loading efficiency was calculated using the following formula:

$$Loading\ Efficiency\,(\%) = \frac{Mass\ of\ HA_{NPs}\,(\mu g)}{Mass\ of\ PLGA_{Total}\,(\mu g)} * 100$$

2.5. Quantitation of HA incorporation and release

The incorporated HA on the surface of the PLGA NPs was quantitated using an ELISA kit specific for HA (Corgenix, Broomfield, CO). To determine the release of HA from the PLGA NPs, 200 µl of these NPs were incubated at 37^{o}C in PBS (pH 7.4) with continuous shaking at 750 rpm. Aliquots of 100 µl were collected at 6 hours and days 1, 3, 7, 14, 21 and 28 and centrifuged at 18,000 ×g for 20 minutes and quantitated using an ELISA kit to determine the sequential amounts of HA released over time.

2.6. Endothelial cell proliferation assay

To evaluate endothelial cell response to HA delivered by PLGA NPs, 600 µl of PLGA or HA-PLGA NPs were mixed with 80 µl collagen type I, 80 µl 10 × PBS and 2 µl 1N NaOH. Sterile double distilled H_2O was added to the mixture to make a final volume of 800 µl. An aliquot of 50 µl of this mixture was delivered to each well of 96-well tissue culture plates and allowed to solidify at 37^{o}C for 1 hour. HMEC-1 (1.0×10^3 cells) were distributed to each well in 100 µl of MCDB-131 medium supplemented with 10% FBS and 1% penicillin-streptomycin. Wells that did not receive cells were used as the baseline control. Number of viable cells was determined between days 3 and 7 using XTT cell proliferation kit II protocol (Roche Applied Science; Indianapolis, IN).

2.7. Endothelial cell growth on HA-PLGA-SIS

SIS and NP modified SIS were prepared in inserts as described previously[145]. PLGA and HA-PLGA NPs were placed onto the mucosal side of SIS at a concentration of 1 mg/ml and incubated on an orbital shaker overnight. HMEC-1 (5.0×10^3 cells/cm^2) were seeded into the inserts; and cell-SIS membranes were harvested between days 3 and 7 after seeding. Genomic DNA was isolated from these preparations using the same protocol as in Chapter 2. Cell growth is indicated by the increasing amount of DNA extracted. Isolated genomic DNA was resolved on 1.2% agarose gels. Images were captured by a gel documentation system (Bio-Rad, Hercules, CA). Genomic DNA band intensities were calculated from the capture images using the Quantity One® image analysis software (Bio-Rad). Genomic DNA from known numbers of HMEC-1 was used as a standard.

2.8. Chicken embryo chorioallantoic membrane (CAM) vascular assay

Fertilized eggs were incubated in a humidified incubator at 37.5^{o}C for 7 days. A 2 cm hole was cut into the superior portion of the shell. Harris Micro Punch sections (1.2 mm) of SIS or NP-SIS were placed onto the CAM near large blood vessels. Antibiotic ointment was applied, holes in the shells were sealed by tape and the eggs were returned for continued incubation. The CAM was fixed in situ for 30 seconds using 4% w/v paraformaldehyde with 0.05% v/v triton X-100 after 4-day incubation. The CAM was excised and chorion was removed. The CAM was then transferred to 6-well culture plates with 4% paraformaldehyde and the vasculature was imaged under a bright field microscope (Wild M400 Photomicroscope) connected to a digital camera (Retiga 1300, Q Imaging, Burnaby BC, CA). Images were captured using the Q Capture software (Q

Imaging, Burnaby BC, CA) at 16× magnification and enhanced via Image J software (NIH).

2.9. Evaluation of angiogenic property of HA-PLGA-SIS in a canine bladder model

Drs. Christopher Roth and Yusuf Kibar (Department of Urology, OUHSC) performed the animal surgeries. Beagle dogs underwent hemicystectomy to remove the upper half of the urinary bladder per our established protocol[28]. A piece of 8 cm × 8 cm of Cook SIS or SIS incubated with 1mg/ml HA-PLGA NPs w:w ratio of 0.5:1 (HA-PLGA-SIS) was used to cover the defect in a watertight fashion after the hemicystectomy. The dogs were euthanized 10 weeks post-operation. The augmented bladders were harvested, inflated with 10% formalin and fixed for 24 hours. The bladders were divided longitudinally and embedded in paraffin. Sections were cut at 5 μm for immunohistochemical analysis[156]. Mason's trichrome was performed to show the structural architecture and phenotype of the tissue. CD31, a blood vessel endothelial marker, was utilized as a primary antibody followed by secondary incubation, chromagen development and light staining with hematoxylin. Total blood vessel count per unit area within the grafts was then determined.

2.10. Statistical analysis

Data were expressed as means ± SD. Statistical differences between multiple experimental groups were analyzed using single factor analysis of variance (ANOVA). If there were significant differences, Student's t-test was used to evaluate the significance between two groups. A statistical difference was considered significant when $p<0.05$.

3. Results

3.1. Characterization of HA-PLGA NPs

The average diameter of synthesized PLGA NPs was 234.6 ± 8.2 nm (n=5) as determined by dynamic light scattering (DLS) (Figure 4-1A). The ζ potential (zeta potential) averaged +42.8 ± 4.3 mV. After surface condensing of HA, the size of HA-PLGA NPs increased to 517.3 ± 6.3 nm (Figure 4-1B) and the zeta potential decreased to +7.79 ± 0.63 mV (Table 4-1). This is critical because the change in ζ potential might interfere in the cell-NPs interaction as most cells are negatively charged. This change in ζ potential could also interfere in the stability of NPs in solution. The morphology and size of these NPs were verified with scanning electron microscopy (SEM) (Figures 4-1A & B).

3.2. HA release from HA-PLGA NPs

HA released from the HA-PLGA NPs was measured between six hrs and 28 days using an ELISA-based quantitation assay. A release rate, ranging from 8.9%/day to 17.6%/day was observed throughout the experimental period (Figure 4-1C). By day 28, 81% of the loaded HA on the NPs had been released. The cumulative release is shown in Figure 4-1D. Both types of release were measured as percentage of initial HA loaded on NPs.

Table 4-1 Characterization of HA-PLGA nanoparticles

Sample	Size (nm)	Polydispersity	Zeta Potential (mV)	Loading Efficiency (%)
PLGA NPs	241.9 ± 8.4	0.062 ± 0.005	+ 34.67 ± 3.98	N/A
HA-PLGA NPs (0.2:1)	436.8 ± 8.5	0.160 ± 0.048	+ 24.48 ± 2.08	15.5
HA-PLGA NPs (0.5:1)	490.3 ± 6.2	0.202 ± 0.012	+ 19.43 ± 1.56	20.4
HA-PLGA NPs (1:1)	517.3 ± 6.3	0.177 ± 0.078	+ 7.79 ± 0.63	26.2

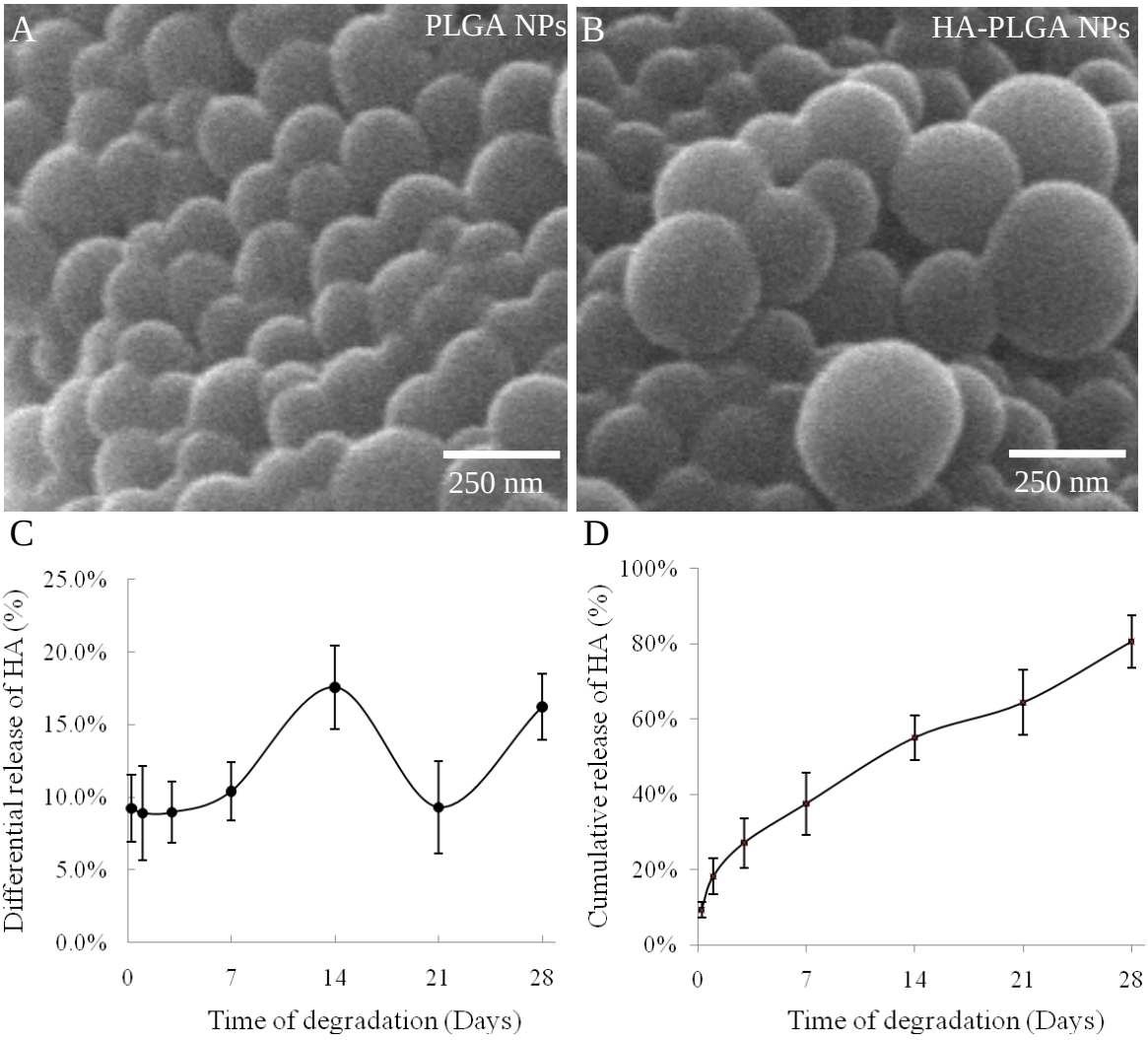

Figure 4-1 SEM of A. PLGA NPs and B. HA-PLGA NPs w:w ratio of 1:1. C. Differential release of HA from HA-PLGA NPs over a period of 28 days (n=3). D. Cumulative release of HA from HA-PLGA NPs. The release was measured as percentage of initial HA loaded on the PLGA NPs. Measurements are reported here as means ± SD.

3.3. Endothelial cell metabolic activity in response to HA-PLGA NPs

Biological effects of HA-PLGA NPs were determined by measuring the metabolic activity of a human microvascular endothelial cell line, HMEC-1, using a XTT cell proliferation kit II (Figure 4-2). HA-PLGA NPs were synthesized using a constant amount of PLGA at 100 µg and varying the HA content to produce three w:w ratios of HA:PLGA (1:1, 0.5:1 and 0.2:1). These HA-PLGA NPs were suspended in collagen gel

and plated into tissue culture plates followed by HMEC-1 cell addition. HMEC-1 responded to 1:1 ratio of HA:PLGA with rapid and significantly elevated metabolic activity, a 7.6-fold increase as compared to a 3.7-fold increase in PLGA NPs alone on day 5 after cell seeding (Figure 4-2). No significant differences were observed on day 7 probably because cells reached full confluence by then. This was expected because confluent cells have limited metabolic activity even if they continue to grow.

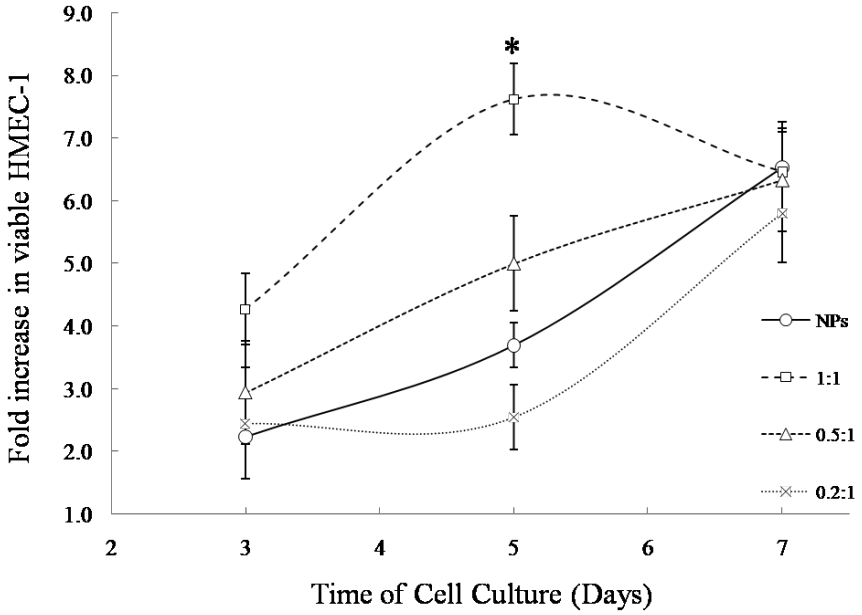

Figure 4-2 Endothelial cell proliferation assay on collagen mixed with NPs and HA-PLGA NPs w:w ratios of 1:1, 0.5:1 and 0.2:1 (n=3). Measurements are reported here as means ± SD. * is where p=0.004 compared to NPs.

3.4. Endothelial cell proliferation on HA-PLGA-SIS

Since SIS is incompatible with radioisotope incorporation, calorimetric assay, or fluorescent assay for measuring cell proliferation, HMEC-1 growth on HA-PLGA-SIS was quantitated by their genomic DNA contents as described before[170] (Figure 4-3A). The HA-PLGA-SIS with 1:1 HA:PLGA w:w ratio supported significantly elevated cell

growth (8.7×10^4 cells) as compared to PLGA-SIS (6.2×10^4 cells) on day 7 following cell seeding (Figure 4-3B).

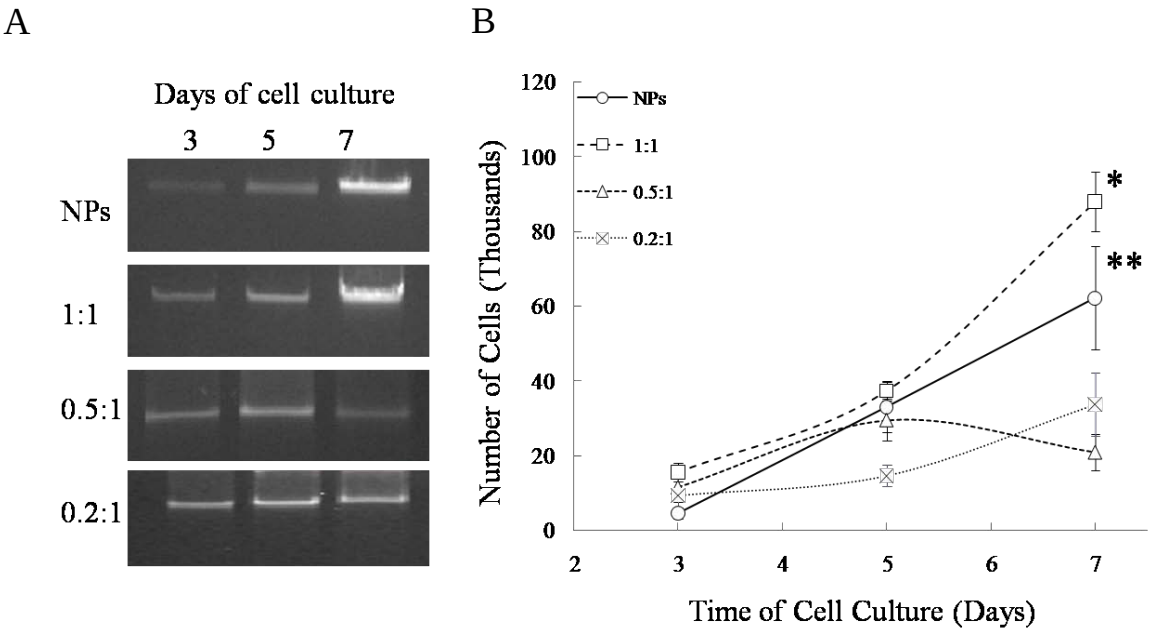

Figure 4-3 Endothelial cell (EC) growth on the SIS modified with nanoparticles (n=3). A. Genomic DNA extractions at days 3, 5 and 7 from HMEC-1 grown on NP-SIS and HA-PLGA-SIS w:w ratios of 1:1, 0.5:1 and 0.2:1. B. HMEC-1 proliferation on the groups mentioned above at different time points. Measurements are reported here as means ± SD. * is where p=0.04 compared to NPs and ** where p=0.02 compared to 0.2:1.

3.5. Chorioallantoic membrane (CAM) angiogenesis assay analysis of HA-PLGA-SIS

CAM has been used as an *in vivo* model to evaluate angiogenic capability of biomaterials[171]. SIS, native and NP-modified, was placed on the CAM near major blood vessels (Figure 4-4A). The total number of blood vessels was counted on images taken on day 5 following biomaterial placements. An average of 45 vessels was observed for HA-PLGA-SIS with HA:PLGA at 1:1 ratio. In contrast, averages of 35, 26 and 23 blood vessels were observed in 0.5:1, 0.2:1 HA:PLGA ratios and PLGA NPs, respectively (Figure 4-4B). No statistical difference was observed between the HA-

PLGA-SIS (0.2:1) and PLGA-SIS. Furthermore, averages of 15 and 9 blood vessels were observed with native SIS and cellulose nitrate, an inert membrane, respectively (Figure 4-4B).

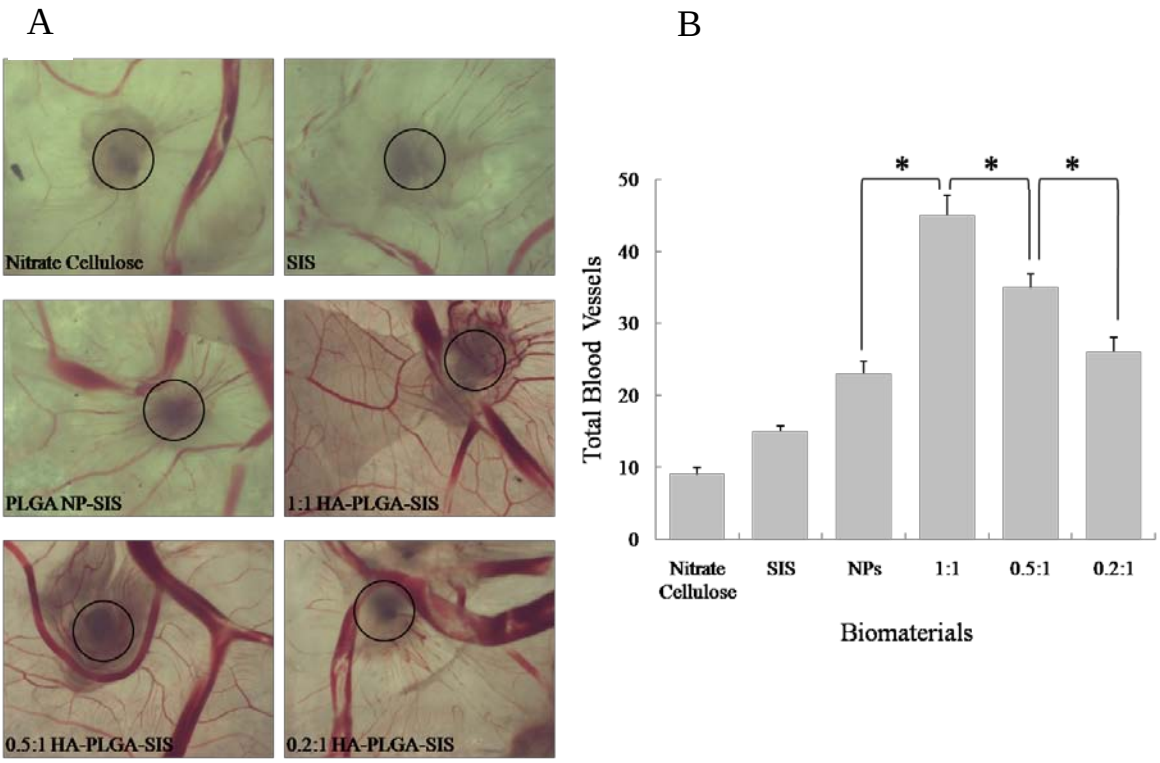

Figure 4-4 A. Effects of the different biomaterials Nitrate Cellulose, SIS, NP-SIS and HA-PLGA-SIS w:w ratios of 1:1, 0.5:1 and 0.2:1 on vascularization as determined by the CAM assay. The circle represents where the biomaterials were implanted. B. Blood vessels were counted manually for the different biomaterials (n=5). Measurements are reported here as means ± SD. * is where $p<0.05$. Original magnification: 16× in all panels.

3.6. Improvement of angiogenesis using HA-PLGA-SIS in a canine bladder model

To evaluate whether HA-PLGA modified SIS can improve angiogenesis in a tissue regeneration model, an established canine bladder augmentation model was used. In Chapter 3 we studied the expression of HA and its receptors in a regenerated rat bladder. The reason a dog bladder model is being used in this study instead because it is bigger than the rat bladder and hence will put to test the potential of the HA-PLGA modified SIS in supporting larger grafts. Dog urinary bladder was subjected to hemicystectomy,

augmented with SIS or HA-PLGA-SIS [SIS incubated with HA:PLGA at 0.5:1 (w:w) ratio overnight on an orbital shaker] and harvested at 10 weeks for histological evaluation. The 10-week time point was picked because the regeneration process has been shown to be completed by then in a previous study[42]. The reason the 0.5:1 HA:PLGA w:w ratio was used, instead of the 1:1 that showed the most significant effect in all *in vitro* and CAM studies, because the animal studies were performed before the *in vitro* studies were completed. Mason's trichrome showed the collagen fibers and smooth muscle bundles in both the graft and native tissues (Figures 4-5A & C). The graft area was identified by the transition from mature smooth muscle bundles in the native tissue to smooth muscle cells and fibers. HA-PLGA-SIS, in general, outperformed SIS in the overall quality of regenerated bladder based on the examination of the regenerated smooth muscle bundles and collagen fibers through Mason's trichrome. Angiogenesis of the graft tissues was determined by immunohistochemical staining with CD31 for endothelial cells (Figures 4-5B & D). Quantitative measurements of CD31 immunoreactive blood vessels demonstrated significantly more blood vessels observed in HA-PLGA-SIS (13.2 ± 3.9 vessels/mm^2) as compared to SIS (6.6 ± 1.6 vessels/mm^2) as shown in Figure 4-5E.

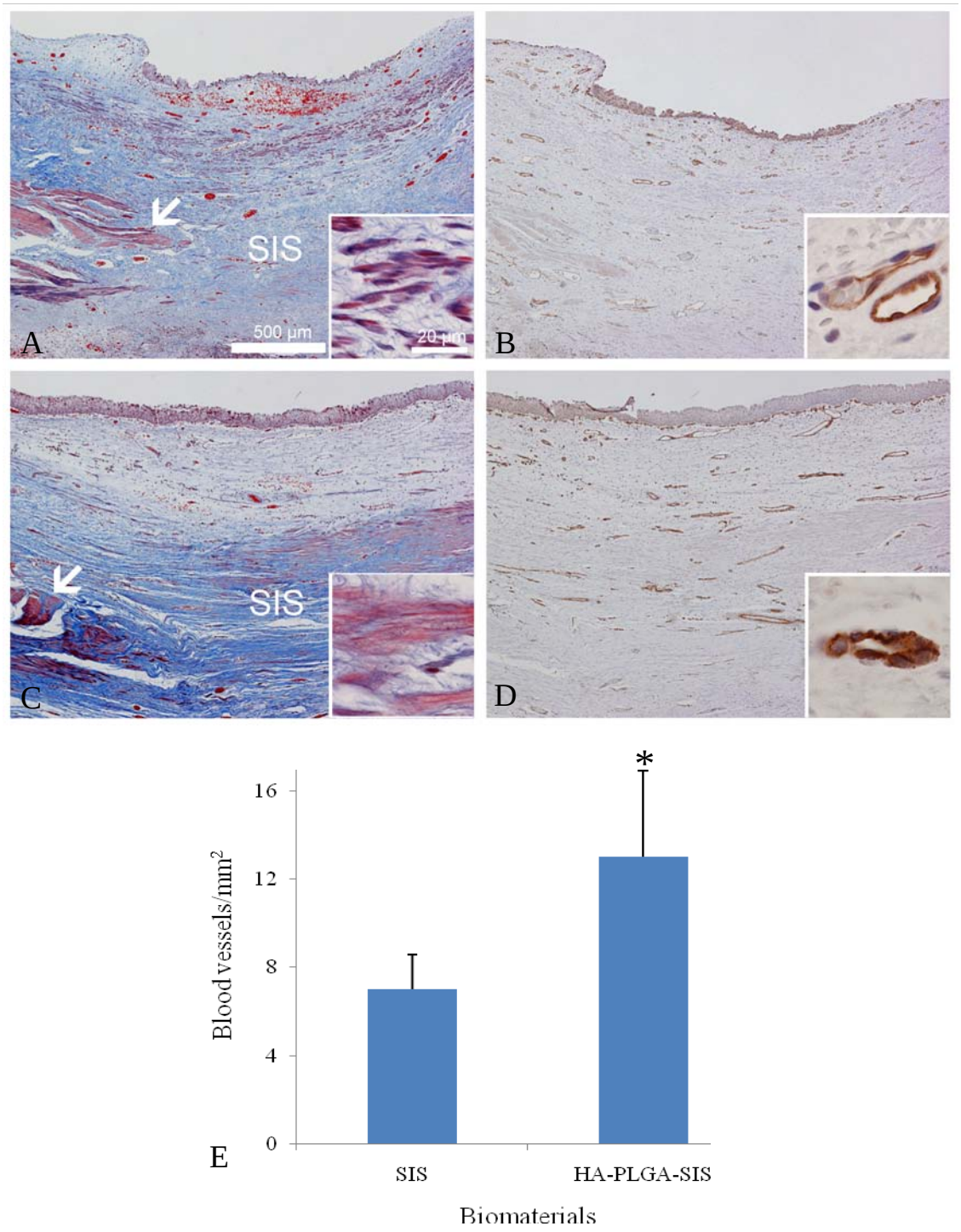

Figure 4-5 Histopathology of the graft in canine urinary bladder was demonstrated by Masson's trichrome stain in A. SIS and C. HA-PLGA-SIS. Note the transition from mature detrusor muscle bundles (arrow, stained red) to developing smooth muscle fibers within the graft area (stained blue). Smaller regenerating muscle fibers are found in the collagenous tissue within the graft (inset). Immunohistochemistry for CD31 was utilized to identify the endothelial cells of blood vessels in the same region in B. SIS and D. HA-PLGA-SIS augmented canine bladder grafts. Blood vessel samples are enlarged in insets. E. Blood vessels were counted manually for the entire graft area (n=5). Measurements are reported here as means ± SD. * is where p=0.01. Original magnification: 4× in main images of panels and 60× in all insets.

4. Discussion

We previously demonstrated that PLGA NPs incorporated into SIS reduced the permeability of the biomaterial to urea and enhanced endothelial cell proliferation without altering the mechanical structure of SIS (Chapter 2). The reduction in urea permeability is particularly important for urinary bladder regeneration since urine leakage may represent a serious obstacle in bladder regeneration. To utilize the biochemical properties of HA to enhance wound healing[111] and angiogenesis[172], HA was encapsulated onto PLGA NPs.

The HA-PLGA NPs were then embedded into SIS to maintain a porous structure and provide a uniform architecture for consistent regenerative properties. Even though cell metabolic activity is not a measure of cell growth, if we take into consideration the combined effect of the enhanced cell metabolic activity and increase in the genomic DNA, we can relate that to an increase in cell growth. The HA-PLGA-SIS not only promoted endothelial cell growth, but also enhanced angiogenesis in both CAM assay and *in vivo* canine bladder augmentation model. We concluded that HA-PLGA-modified SIS might overcome the heterogeneity of naturally derived biomaterials and promote the establishment of vascular networks crucial to rapid and complete tissue regeneration.

PLGA NPs have several advantages over other delivery methods such as liposomes based on their stability, high encapsulation efficiency, and better control over the release of the encapsulated therapeutic molecules[173] simply by controlling the monomer ratio, molecular weight as well as other parameters. In addition size, surface charge, hydrophilicity and degradation rate of NPs can be optimized[65]. The PLGA NPs were synthesized using a modified double-emulsion method to produce positively charged

NPs. This feature gives the NPs the unique ability to condense negatively charged molecules, such as HA, on their surface. The biodegradable characteristics of PLGA NPs make it feasible to deliver molecules of interest in moderate portions in a continuous mode without leaving any toxic byproducts. Although PLGA NPs are small enough to be internalized into cells if needed[70], giving them advantage over larger systems, HA was encapsulated outside of PLGA in this application so that cells expressing HA receptors can interact with the HA. In other words, the HA did not need to be internalized inside the cells to have an effect. Most HA cell surface receptors are located on the cell membrane that constantly interact with the HA that is outside the cell in the ECM, for example.

One might point to a concern that the HA-PLGA NPs with w:w ratio of 1:1 might be too big (517.3 nm from Table 4-1) to embed into the SIS and hence would not be able to reduce the permeability of the SIS to urea. We found earlier in Chapter 2 that 300 nm size spheres reduced the permeability of SIS to urea the most whereas 500 nm not so much. The reason there is a difference in diameter between the HA-PLGA NPs with w:w ratio of 1:1 in the SEM images (Figure 4-1B) and Table 4-1 is because the DLS measures the hydrodynamic diameters, which include the NPs as well as the water molecules surrounding the particles. The diameters obtained from the SEM, on the other hand are the "dry" diameters. Hence, the diameter measured by the DLS of a nanoparticle solution appeared to be bigger than that measured by SEM of a dry sample. The dry diameters of PLGA and HA-PLGA NPs were 156 nm and 328 nm, respectively.

As mentioned earlier, the negatively charged HA was condensed on the surface of the positively charged PLGA NPs. It is this electrostatic attraction between HA and PLGA

that kept HA conjugated to the surface. HA is a linear polysaccharide however, in solution, HA has a secondary structure because of the hydrogen bonding making it behave as an expanded coil with diameter of 500 nm[174]. Trimm and Jennings showed that each disaccharide unit is almost equivalent to 1 nm[175]. HA below 500 kDa shows a rod-like behavior and above that molecular weight behaves as a random coil[175]. In addition, X-ray diffraction of potassium hyaluronate fiber showed a left-handed 4-fold helix of axial rise 0.95 nm per disaccharide[176]. Therefore, we can say the 74 kDa HA (185 disaccharide units) used in this study is roughly 185 nm in length. From the difference in SEM "dry" diameters between PLGA and HA-PLGA NPs we can say that the thickness of the HA layer around the PLGA NPs is about 172 nm. We propose the following mechanism of HA binding to the PLGA NPs. Similar to the binding of the negatively charged DNA to the positively charged histones, the HA could wrap around the PLGA NPs as a string wraps around a marble. However, unlike the DNA binding which is more organized, the binding of HA to PLGA could be random. Therefore, it could be very possible that the HA-PLGA binding may not completely follow the DNA-histone mechanism but may in fact be a combination of HA wrapping around the PLGA NPs as well as HA sticking outward.

HA has been shown to play a critical role in cell growth and differentiation[177] and to elicit angiogenic responses. Angiogenic property of HA appears to be size related[178]. One of the unique features of HA is that native or high molecular weight HA can be enzymatically cleaved to produce fragment sizes of HA (oligo HA, o-HA)[172] that are pro-angiogenic. In some cases, as in inflammation and angiogenesis, long (400-2000 kDa) and short chain-size (~ 2.4-8 kDa) HA effects are antagonistic[127]. West et al.

demonstrated that HA fragments of 4-25 disaccharides (~ 1.6-10 kDa) were angiogenic[98]. In this study, we used an intermediate size HA fragment with an average molecular weight of 74 kDa (about 185 disaccharide units). Future studies will explore various size fragments and concentrations of HA to produce reliable SIS for consistent regenerative properties.

HA was utilized for enhancing regenerative properties of SIS, since it is a sugar-based ECM component and has a longer shelf life than angiogenic protein molecules such as vascular endothelial growth factor (VEGF) or fibroblast growth factor (FGF). Elevated levels of HA have been identified in the ECM of the fetus and have been correlated with scarless wound healing with rapid but organized collagen deposition[179]. Cabrera et al. showed that rat wounds treated with hyaluronan associated protein-collagen complex healed quickly with more organized collagen as compared to untreated wounds[180]. They concluded that manipulation of adult wound scarring might be feasible using proteins present in fetal skin. HA has also been shown to inhibit platelet aggregation and cytokine release, which may explain, in part, the minimal inflammation and scarless healing characteristic of fetal dermal repair[181]. In this report, we provided an approach for controlled incorporation and release of HA into SIS for enhanced angiogenesis that is required for optimal tissue regeneration.

Angiogenesis is critical for supporting complete tissue engineering, as blood vessels are needed to deliver oxygen and nutrients to the new tissue and remove byproducts of metabolism. Both cell models and *in vivo* models were used to determine the effectiveness of the HA-PLGA NPs modified SIS on endothelial cell growth and angiogenesis. However, optimal levels of angiogenesis in tissue regeneration are not yet

defined. Even though the 1:1 w:w ratio of HA:PLGA showed the most significant effect in enhancing cell growth and angiogenesis, we decided to study the effect of the 0.5:1 ratio in the dog bladder model. This is unfortunately one of the study limitations. The reason 0.5:1 was chosen because at the time of the animal study, the *in vitro* studies have not been completed yet. There was a concern that the 1:1 HA:PLGA might be very potent. Overgrowth or uncontrolled proliferation of vasculature may lead to arteriovenous malformation or even tumorigenesis. Another concern was that the 0.2:1 might not have enough HA to trigger any response as determined by experiments discussed earlier. Therefore, although HA-PLGA at 1:1 and 0.5:1 (w:w) showed significant improvements in promoting endothelial cell growth and angiogenesis in CAM, we chose to utilize the 0.5:1 (w:w) HA:PLGA ratio instead of the 1:1 (w:w) in the dog bladder augmentation model based on moderate angiogenesis that occurred with this ratio in the CAM model. Future studies are required to compare various ratios of HA and PLGA in their ability to promote angiogenesis and to define the most consistent and reliable biomaterial for tissue engineering. Furthermore, although we have chosen to utilize a dog bladder augmentation model to study *in vivo* effects of HA-PLGA-SIS, the benefits of this biomaterial will apply to other areas of regenerative medicine including abdominal wall reconstruction, nerve grafting, and skin replacement.

Unfortunately, there were limitations in this study. One of which is failure to include an appropriate proper control (PLGA NPs modified SIS) in the *in vivo* animal model. This would have allowed us to determine if the angiogenic potential of HA-PLGA NPs modified SIS was due to the HA alone or to the PLGA NPs alone or a combined effect. In Chapter 2 we showed that PLGA NPs on their own can enhance endothelial cell

growth on the SIS as compared to unmodified SIS. Therefore, we cannot say that HA enhanced the angiogenic potential of the SIS because it might be a pure effect of the PLGA NPs. Another limitation was the use of HMEC-1 cells at early passages (12-14) as opposed to late passages (20-22) that were used earlier in similar experiments in Chapter 2. This was evident by the fact that Genomic DNA extracted from HMEC-1 growing on PLGA SIS showed 2-3× cell increase as compared to the same experiments performed earlier with the same type of HMEC-1 cells (but a much later passage as discussed above). Therefore, it is very critical to use cells at early passages for similar studies. The experiments performed in these studies used similar passage cells for all groups per study. Another study limitation is the fact that there were no commercially available antibodies for dog tissue. We could not determine expression of HA and its receptors in a regenerated dog bladder. Future studies should focus on generating antibodies against dog tissue to validate that the results obtained could be due to delivery of exogenous HA.

In conclusion, the HA-PLGA NPs modified SIS supported HMEC-1 growth and enhanced the angiogenic potential of the newly designed biomaterial both *in vitro* with the CAM model and *in vivo* with the dog bladder augmentation model. We have proven that the incorporation of NPs into naturally derived biomaterials such as SIS can reduce the heterogeneity of the biomaterial and enhance its regenerative properties.

Chapter 5 Overall Conclusion & Future Direction

The long-term goal of this study is to introduce the utility of nanotechnology in biomaterials to develop a consistent off-the-shelf scaffold that can recruit and sustain a normally functioning endothelium that is critical in tissue regeneration. Endothelial cells have an important role in the wound healing process. A healthy vascular supply is critical to restore the endothelial cell signaling pathways that are altered by injury and disease. It is believed that this modified biomaterial can be applied in various clinical scenarios where vascularization is altered.

Heterogeneity of SIS presents a major issue for this biomaterial to produce consistent tissue repair and regeneration. We demonstrated that the introduction of NPs represents a potential solution to improve the quality of regenerated tissues like urinary bladder using SIS. Nanoparticles with size range 200-500 nm can be embedded into the SIS to reduce the permeability of SIS to urea. The enhanced HMEC-1 cell proliferation on PLGA NP modified SIS, which may result from a uniformed porous structure as compared to unmodified SIS, led to enhanced angiogenesis *in vitro*. To take this one-step further, these PLGA NPs can serve as potential carriers for angiogenic factors such as HA. However, before delivery of exogenous HA can be performed, HA receptors must be available. Therefore, expression of HA and HA receptors in regenerated tissue must be determined. Hence, it is very important to determine antibodies that can detect HA and its receptors in a dog bladder model. This will validate the delivery of HA and show that in fact it is the interactions of exogenous HA with its receptors that are responsible for the enhanced angiogenic effect of the newly modified biomaterial.

We have sought to study the temporal expression of HA and its receptors in a regenerated animal model. Our study was the first to demonstrate changes in the deposition of HA and temporal expression of HA receptors during the process of rat urinary bladder regeneration. We showed that HA and its two major receptors, CD44 and LYVE-1, co-expressed in a temporal fashion. Expression of HA and HA receptors could be closely related to inflammatory responses, cell differentiation, angiogenesis and lymphangiogenesis during different phases of tissue regeneration. Further research is needed to determine the mechanism of expression of HA-induced bladder regeneration to improve the outcomes in tissue engineering. For example, to understand fully the cell signaling mechanism behind the effect of HA, one might look into blocking one HA receptor at a time and perform a western blot to determine the protein expression. We can also study the expression of the HA receptors after incorporation of exogenous HA.

HA-PLGA nanoparticles were synthesized to modify even further a naturally derived biomaterial, SIS, for enhanced tissue regeneration. Biodegradable PLGA NPs serve as an excellent vehicle for delivering biological molecules. From *in vitr*o to *in vivo* models, NP-modified biomaterial design has demonstrated the capacity of HA-PLGA NPs to enhance endothelial cell proliferation and ultimately promote angiogenesis in a pre-clinical large animal bladder augmentation model. This newly modified SIS (HA-PLGA-SIS) could serve as the future biomaterial needed for better tissue regeneration. As stated before, since species difference can be an issue (rat vs. dog), we must first show that HA and its receptors are available throughout the regeneration process.

Recall that the SIS was harvested from 3-year old pigs. One avenue of exploration would be to perform experiments on SIS taken from different pigs of different sizes and

ages. Furthermore, one can explore SIS harvested from different locations of the small intestine within the same pig and study the effect of embedding PLGA NPs into these materials. It would be interesting to see if all of the above-mentioned materials would display the same permeability to urea, after being modified by PLGA NPs.

Another avenue to explore is testing different sizes (molecular weights) of HA. Scientists do not fully understand why different sizes of HA have opposite roles nor can they determine a critical size or borderline. We have shown that HA with an average molecular weight of 74 kDa showed promising angiogenic potential both *in vitro* and *in vivo*. However, further investigations need to be performed to determine the optimal size and concentration of HA before any clinical trials.

Literature Cited

1. Skalak R & Fox CF. *Tissue Engineering*, (Liss. New York, 1988).
2. Staack A, Hayward SW, Baskin LS & Cunha GR. Molecular, Cellular and Developmental Biology of Urothelium as a Basis of Bladder Regeneration. *Differentiation* 73, 121-133 (2005).
3. Venn S & Mundy T. Bladder Reconstruction: Urothelial Augmentation, Trauma, Fistula. *Curr Opin Urol* 12, 201-203 (2002).
4. Duel BP, Gonzalez R & Barthold JS. Alternative Techniques for Augmentation Cystoplasty. *J Urol* 159 998-1005 (1998).
5. Gurocak S, De Gier RP & Feitz W. Bladder Augmentation without Integration of Intact Bowel Segments: Critical Review and Future Perspectives. *J Urol* 177, 839-844 (2007).
6. Kudish HG. The Use of Polyvinyl Sponge for Experimental Cystoplasty. *J Urol* 78, 232-235 (1957).
7. Ashkar L & Heller E. The Silastic Bladder Patch. *J Urol* 98, 679-683 (1967).
8. Kelami A, Dustmann HO, Ludtke-Handjery A, Carcamo V & Herlld G. Experimental Investigations of Bladder Regeneration Using Teflon-Felt as a Bladder Wall Substitute. *J Urol* 104, 693-698 (1970).
9. Kelami A. Lyophilized Human Dura as a Bladder Wall Substitute: Experimental and Clinical Results. *J Urol* 105, 518-522 (1971).
10. Pattison MA, Wurster S, Webster TJ & Haberstroh KM. Three-Dimensional, Nano-Structured Plga Scaffolds for Bladder Tissue Replacement Applications. *Biomaterials* 26, 2491-2500 (2005).
11. Atala A, Bauer SB, Soker S, Yoo JJ & Retik AB. Tissue-Engineered Autologous Bladders for Patients Needing Cystoplasty. *Lancet* 367, 1241-1246 (2006).
12. Novick AC, Straffon RA, Koshino I, Banowsky LH, Levin H & Kambic H. Experimental Bladder Substitution Using a Biodegradable Graft of Natural Tissue. *J Biomed Mater Res* 12, 125-147 (1978).
13. Nakanishi Y, Chen G, Komuro H, Ushida T, Kaneko S, Tateishi T & Kaneko M. Tissue-Engineered Urinary Bladder Wall Using Plga Mesh-Collagen Hybrid Scaffolds: A Comparison Study of Collagen Sponge and Gel as a Scaffold. *Journal of pediatric surgery* 38, 1781-1784 (2003).
14. Oh SH, Ward CL, Atala A, Yoo JJ & Harrison BS. Oxygen Generating Scaffolds for Enhancing Engineered Tissue Survival. *Biomaterials* 30, 757-762 (2009).

15. Cilento BG, Freeman MR, Schneck FX, Retik AB & Atala A. Phenotypic and Cytogenetic Characterization of Human Bladder Urothelia Expanded in Vitro. *J Urol* 152, 665-670 (1994).

16. Yoo JJ, Meng J, Oberpenning F & Atala A. Bladder Augmentation Using Allogenic Bladder Submucosa Seeded with Cells. *Urology* 51, 221-225 (1998).

17. Oberpenning F, Meng J, Yoo JJ & Atala A. De Novo Reconstitution of a Functional Mammalian Urinary Bladder by Tissue Engineering. *Nature biotechnology* 17, 149-155 (1999).

18. Badylak SF, Lantz GC, Coffey A & Geddes LA. Small Intestinal Submucosa as a Large Diameter Vascular Graft in the Dog. *J Surg Res* 47, 74-80 (1989).

19. Androjna C, Spragg RK & Derwin KA. Mechanical Conditioning of Cell-Seeded Small Intestine Submucosa: A Potential Tissue-Engineering Strategy for Tendon Repair. *Tissue Eng* (2007).

20. Hiles MC, Badylak SF, Lantz GC, Kokini K, Geddes LA & Morff RJ. Mechanical Properties of Xenogeneic Small-Intestinal Submucosa When Used as an Aortic Graft in the Dog. *J Biomed Mater Res* 29, 883-891 (1995).

21. Badylak SF, Lantz GC, Coffey A & Geddes LA. Small Intestinal Submucosa as a Large Diameter Vascular Graft in the Dog. *J.Surg.Res.* 47, 74-80 (1989).

22. Kim MS, Hong KD, Shin HW, Kim SH, Kim SH, Lee MS, Jang WY, Khang G & Lee HB. Preparation of Porcine Small Intestinal Submucosa Sponge and Their Application as a Wound Dressing in Full-Thickness Skin Defect of Rat. *International journal of biological macromolecules* 36, 54-60 (2005).

23. Clarke KM, Lantz GC, Salisbury SK, Badylak SF, Hiles MC & Voytik SL. Intestine Submucosa and Polypropylene Mesh for Abdominal Wall Repair in Dogs. *J.Surg.Res.* 60, 107-114 (1996).

24. Caione P, Capozza N, Zavaglia D, Palombaro G & Boldrini R. In Vivo Bladder Regeneration Using Small Intestinal Submucosa: Experimental Study. *Pediatr Surg Int* 22, 593-599 (2006).

25. Zhang Y, Kropp BP, Lin HK, Cowan R & Cheng EY. Bladder Regeneration with Cell-Seeded Small Intestinal Submucosa. *Tissue Eng* 10, 181-187 (2004).

26. Prevel CD, Eppley BL, Summerlin DJ, Sidner R, McCarty M & Badylak SF. Small Intestinal Submucosa: Utilization as a Wound Dressing in Full-Thickness Rodent Wounds. *Ann.Plast.Surg.* 35, 381-388 (1995).

27. Gubbels SP, Richardson M, Trune D, Bascom DA & Wax MK. Tracheal Reconstruction with Porcine Small Intestine Submucosa in a Rabbit Model. *Otolaryngol Head Neck Surg* 134, 1028-1035 (2006).

28. Badylak SF, Kropp B, McPherson T, Liang H & Snyder PW. Small Intestinal Submucosa: A Rapidly Resorbed Bioscaffold for Augmentation Cystoplasty in a Dog Model. *Tissue Eng* 4, 379-387 (1998).

29. Vaught JD, Kropp BP, Sawyer BD, Rippy MK, Badylak SF, Shannon HE & Thor KB. Detrusor Regeneration in the Rat Using Porcine Small Intestinal Submucosal Grafts: Functional Innervation and Receptor Expression. *J.Urol.* 155, 374-378 (1996).

30. Kropp BP, Rippy MK, Badylak SF, Adams MC, Keating MA, Rink RC & Thor KB. Regenerative Urinary Bladder Augmentation Using Small Intestinal Submucosa: Urodynamic and Histopathologic Assessment in Long-Term Canine Bladder Augmentations. *J.Urol.* 155, 2098-2104 (1996).

31. Kropp BP, Sawyer BD, Shannon HE, Rippy MK, Badylak SF, Adams MC, Keating MA, Rink RC & Thor KB. Characterization of Small Intestinal Submucosa Regenerated Canine Detrusor: Assessment of Reinnervation, in Vitro Compliance and Contractility. *J.Urol.* 156, 599-607 (1996).

32. Pope JCI, Davis MM, Smith ER, Jr., Walsh MJ, Ellison PK, Rink RC & Kropp BP. The Ontogeny of Canine Small Intestinal Submucosa Regenerated Bladder. *J.Urol.* 158, 1105-1110 (1997).

33. Shalhav AL, Elbahnasy AM, Bercowsky E, Kovacs G, Brewer A, Maxwell KL, McDougall EM & Clayman RV. Laparoscopic Replacement of Urinary Tract Segments Using Biodegrable Materials in a Large-Animal Model. *J.Endourol.* 13, 241-244 (1999).

34. Dahms SE, Piechota HJ, Nunes L, Dahiya R, Lue TF & Tanagho EA. Free Ureteral Replacement in Rats: Regeneration of Ureteral Wall Components in the Acellular Matrix Graft. *Urology* 50, 818-825 (1997).

35. Cheng EY & Kropp BP. Urologic Tissue Engineering with Small-Intestinal Submucosa: Potential Clinical Applications. *World journal of urology* 18, 26-30 (2000).

36. Pu LL. Small Intestinal Submucosa (Surgisis) as a Bioactive Prosthetic Material for Repair of Abdominal Wall Fascial Defect. *Plastic and reconstructive surgery* 115, 2127-2131 (2005).

37. Ho KL, Witte MN & Bird ET. 8-Ply Small Intestinal Submucosa Tension-Free Sling: Spectrum of Postoperative Inflammation. *J Urol* 171, 268-271 (2004).

38. Petter-Puchner AH, Fortelny RH, Mittermayr R, Walder N, Ohlinger W & Redl H. Adverse Effects of Porcine Small Intestine Submucosa Implants in Experimental Ventral Hernia Repair. *Surg Endosc* 20, 942-946 (2006).

39. Ansaloni L, Catena F, Coccolini F, Gazzotti F, D'Alessandro L & Daniele Pinna A. Inguinal Hernia Repair with Porcine Small Intestine Submucosa: 3-Year Follow-up Results of a Randomized Controlled Trial of Lichtenstein's Repair with Polypropylene Mesh Versus Surgisis Inguinal Hernia Matrix. *American journal of surgery* (2009).

40. Kropp BP, Eppley BL, Prevel CD, Rippy MK, Harruff RC, Badylak SF, Adams MC, Rink RC & Keating MA. Experimental Assessment of Small

Intestinal Submucosa as a Bladder Wall Substitute. *Urology* 46, 396-400 (1995).

41. Vaught JD, Kropp BP, Sawyer BD, Rippy MK, Badylak SF, Shannon HE & Thor KB. Detrusor Regeneration in the Rat Using Porcine Small Intestinal Submucosal Grafts: Functional Innervation and Receptor Expression. *J Urol* 155, 374-378 (1996).

42. Kropp BP, Cheng EY, Lin HK & Zhang Y. Reliable and Reproducible Bladder Regeneration Using Unseeded Distal Small Intestinal Submucosa. *J Urol* 172, 1710-1713 (2004).

43. Raghavan D, Kropp BP, Lin HK, Zhang Y, Cowan R & Madihally SV. Physical Characteristics of Small Intestinal Submucosa Scaffolds Are Location-Dependent. *J Biomed Mater Res A* 73, 90-96 (2005).

44. Panyam J & Labhasetwar V. Biodegradable Nanoparticles for Drug and Gene Delivery to Cells and Tissue. *Adv Drug Deliv Rev* 55, 329-347 (2003).

45. Lee SJ, Jeong JR, Shin SC, Kim JC, Chang YH, Chang YM & Kim JD. Nanoparticles of Magnetic Ferric Oxides Encapsulated with Poly(D,L Latide-Co-Glycolide) and Their Applications to Magnetic Resonance Imaging Contrast Agent. *J. Magn. Magn. Mater.* 272-76, 2432-2433 (2004).

46. Labhasetwar V, Song C, Humphrey W, Shebuski R & Levy RJ. Arterial Uptake of Biodegradable Nanoparticles: Effect of Surface Modifications. *J Pharm Sci* 87, 1229-1234 (1998).

47. Liu H, Finn N & Yates MZ. Encapsulation and Sustained Release of a Model Drug, Indomethacin, Using Co(2)-Based Microencapsulation. *Langmuir* 21, 379-385 (2005).

48. Zweers MLT, Engbers GHM, Grijpma DW & Feijen J. Release of Anti-Restenosis Drugs from Poly(Ethylene Oxide)-Poly (Dl-Lactic-Co-Glycolic Acid) Nanoparticles. *J Control Release* 114, 317-324 (2006).

49. Yuan XD, Li L, Rathinavelu A, Hao JS, Narasimhan M, He M, Heitlage V, Tam L, Viqar S & Salehi M. Sirna Drug Delivery by Biodegradable Polymeric Nanoparticles. *Journal of Nanoscience and Nanotechnology* 6, 2821-2828 (2006).

50. Leo E, Scatturin A, Vighi E & Dalpiaz A. Polymeric Nanoparticles as Drug Controlled Release Systems: A New Formulation Strategy for Drugs with Small or Large Molecular Weight. *J Nanosci Nanotechnol* 6, 3070-3079 (2006).

51. Shakweh M & Fattal E. Design and Characterisation of Poly(Lactide-Co-Glycolide) Small Particulate Systems for the Delivery of Immunostimulant Cpg Oligonucleotide. *J Nanosci Nanotechnol* 6, 2811-2820 (2006).

52. Yi F, Wu H & Jia GL. Formulation and Characterization of Poly (D,L-Lactide-Co-Glycolide) Nanoparticle Containing Vascular Endothelial Growth Factor for Gene Delivery. *J Clin Pharm Ther* 31, 43-48 (2006).

53. Oster CG, Wittmar M, Bakowsky U & Kissel T. DNA Nano-Carriers from Biodegradable Cationic Branched Polyesters Are Formed by a Modified Solvent Displacement Method. *Journal of Controlled Release* 111, 371-381 (2006).

54. Hillaireau H, Le Doan T & Couvreur P. Polymer-Based Nanoparticles for the Delivery of Nucleoside Analogues. *J Nanosci Nanotechnol* 6, 2608-2617 (2006).

55. Yang J, Song C, Sun H, Wu L, Tang L, Leng X, Wang P, Xu Y, Li Y & Guan H. [Polymeric Nanoparticles with Therapeutic Gene for Gene Therapy: I. Preparation and in Vivo Gene Transfer Study]. *Sheng Wu Yi Xue Gong Cheng Xue Za Zhi* 22, 438-442 (2005).

56. Ribeiro S, Hussain N & Florence AT. Release of DNA from Dendriplexes Encapsulated in Plga Nanoparticles. *Int J Pharm* 298, 354-360 (2005).

57. Hariharan S, Bhardwaj V, Bala I, Sitterberg J, Bakowsky U & Kumar M. Design of Estradiol Loaded Plga Nanoparticulate Formulations: A Potential Oral Delivery System for Hormone Therapy. *Pharmaceutical Research* 23, 184-195 (2006).

58. Zeisser-Labouebe M, Lange N, Gurny R & Delie F. Hypericin-Loaded Nanoparticles for the Photodynamic Treatment of Ovarian Cancer. *International Journal of Pharmaceutics* 326, 174-181 (2006).

59. Farokhzad OC, Cheng JJ, Teply BA, Sherifi I, Jon S, Kantoff PW, Richie JP & Langer R. Targeted Nanoparticle-Aptamer Bioconjugates for Cancer Chemotherapy in Vivo. *Proc Natl Acad Sci U S A* 103, 6315-6320 (2006).

60. Win KY & Feng SS. Effects of Particle Size and Surface Coating on Cellular Uptake of Polymeric Nanoparticles for Oral Delivery of Anticancer Drugs. *Biomaterials* 26, 2713-2722 (2005).

61. Saxena V, Sadoqi M & Shao J. Polymeric Nanoparticulate Delivery System for Indocyanine Green: Biodistribution in Healthy Mice. *International Journal of Pharmaceutics* 308, 200-204 (2006).

62. Davda J & Labhasetwar V. Characterization of Nanoparticle Uptake by Endothelial Cells. *Int J Pharm* 233, 51-59 (2002).

63. Gu F, Zhang L, Teply BA, Mann N, Wang A, Radovic-Moreno AF, Langer R & Farokhzad OC. Precise Engineering of Targeted Nanoparticles by Using Self-Assembled Biointegrated Block Copolymers. *Proc Natl Acad Sci U S A* 105, 2586-2591 (2008).

64. He X, Ma J, Mercado AE, Xu W & Jabbari E. Cytotoxicity of Paclitaxel in Biodegradable Self-Assembled Core-Shell Poly(Lactide-Co-Glycolide Ethylene Oxide Fumarate) Nanoparticles. *Pharm Res* 25, 1552-1562 (2008).

65. Astete CE & Sabliov CM. Synthesis and Characterization of Plga Nanoparticles. *Journal of biomaterials science* 17, 247-289 (2006).

66. Cohen-Sela E, Chorny M, Koroukhov N, Danenberg HD & Golomb G. A New Double Emulsion Solvent Diffusion Technique for Encapsulating Hydrophilic Molecules in Plga Nanoparticles. *J Control Release* 133, 90-95 (2009).

67. Sahana DK, Mittal G, Bhardwaj V & Kumar MN. Plga Nanoparticles for Oral Delivery of Hydrophobic Drugs: Influence of Organic Solvent on Nanoparticle Formation and Release Behavior in Vitro and in Vivo Using Estradiol as a Model Drug. *J Pharm Sci* 97, 1530-1542 (2008).

68. Ngaboni Okassa L, Marchais H, Douziech-Eyrolles L, Cohen-Jonathan S, Souce M, Dubois P & Chourpa I. Development and Characterization of Sub-Micron Poly(D,L-Lactide-Co-Glycolide) Particles Loaded with Magnetite/Maghemite Nanoparticles. *Int J Pharm* 302, 187-196 (2005).

69. Astete CE & Sabliov CM. Synthesis of Poly(Dl-Lactide-Co-Glycolide) Nanoparticles with Entrapped Magnetite by Emulsion Evaporation Method. *Particulate Science and Technology* 24, 321-328 (2006).

70. Panyam J & Labhasetwar V. Dynamics of Endocytosis and Exocytosis of Poly(D,L-Lactide-Co-Glycolide) Nanoparticles in Vascular Smooth Muscle Cells. *Pharm Res* 20, 212-220 (2003).

71. Hidaka C, Ibarra C, Hannafin JA, Torzilli PA, Quitoriano M, Jen SS, Warren RF & Crystal RG. Formation of Vascularized Meniscal Tissue by Combining Gene Therapy with Tissue Engineering. *Tissue Eng* 8 93-105 (2002).

72. Suzuki N, Takahashi S & Okabe S. Relationship between Vascular Endothelial Growth Factor and Angiogenesis in Spontaneous and Indomethacin-Delayed Healing of Acetic Acid-Induced Gastric Ulcers in Rats. *J Physiol Pharmacol* 49 515-527 (1998).

73. Greenhalgh DG, Sprugel KH, Murray MJ & Ross R. Pdgf and Fgf Stimulate Wound Healing in the Genetically Diabetic Mouse. *The American journal of pathology* 136, 1235-1246 (1990).

74. Carmeliet P, Ferreira V, Breier G, Pollefeyt S, Kieckens L, Gertsenstein M, Fahrig M, Vandenhoeck A, Harpal K, Eberhardt C, Declercq C, Pawling J, Moons L, Collen D, Risau W & Nagy A. Abnormal Blood Vessel Development and Lethality in Embryos Lacking a Single Vegf Allele. *Nature* 380, 435-439 (1996).

75. Ferrara N, Carver-Moore K, Chen H, Dowd M, Lu L, O'Shea KS, Powell-Braxton L, Hillan KJ & Moore MW. Heterozygous Embryonic Lethality Induced by Targeted Inactivation of the Vegf Gene. *Nature* 380, 439-442 (1996).

76. Rio MD, Larcher F, Meana A, Segovia J, Alvarez A & Jorcano J. Nonviral Transfer of Genes to Pig Primary Keratinocytes. Induction of Angiogenesis by Composite Grafts of Modified Keratinocytes Overexpressing Vegf Driven by a Keratin Promoter. *Gene Ther* 6, 1734-1741 (1999).

77. Arnoczky SP, Warren RF & Spivak JM. Meniscal Repair Using an Exogenous Fibrin Clot. An Experimental Study in Dogs. *J Bone Joint Surg Am* 70 1209-1217 (1988).

78. Gershuni DH, Skyhar MJ, Danzig LA, Camp J, Hargens AR & Akeson WH. Experimental Models to Promote Healing of Tears in the Avascular Segment of Canine Knee Menisci. *J.Bone Joint Surg.Am.* 71 1363-1370 (1989).

79. Hashimoto J, Kurosaka M, Yoshiya S & Hirohata K. Meniscal Repair Using Fibrin Sealant and Endothelial Cell Growth Factor. An Experimental Study in Dogs. *Am J Sports Med* 20 537-541 (1992).

80. Okuda K, Ochi M, Shu N & Uchio Y. Meniscal Rasping for Repair of Meniscal Tear in the Avascular Zone. *Arthroscopy* 15, 281-286 (1999).

81. Stone KR, Steadman JR, Rodkey WG & Li ST. Regeneration of Meniscal Cartilage with Use of a Collagen Scaffold. Analysis of Preliminary Data. *J Bone Joint Surg Am* 79 1770-1777 (1997).

82. Del Rio M, Larcher F, Meana A, Segovia J, Alvarez A & Jorcano J. Nonviral Transfer of Genes to Pig Primary Keratinocytes. Induction of Angiogenesis by Composite Grafts of Modified Keratinocytes Overexpressing Vegf Driven by a Keratin Promoter. *Gene Ther* 6, 1734-1741 (1999).

83. Ibrahim S & Ramamurthi A. Hyaluronic Acid Cues for Functional Endothelialization of Vascular Constructs. *Journal of tissue engineering and regenerative medicine* 2, 22-32 (2008).

84. Dvorak HF, Nagy JA, Feng D, Brown LF & Dvorak AM. Vascular Permeability Factor/Vascular Endothelial Growth Factor and the Significance of Microvascular Hyperpermeability in Angiogenesis. *Curr Top Microbiol Immunol* 237, 97-132 (1999).

85. Brown LF, Detmar M, Claffey KP, Nagy JA, Feng D, Dvorak AM & Dvorak HF. Vascular Permeability Factor/Vascular Endothelial Growth Factor: A Multifunctional Angiogenic Cytokine. *EXS.* 79, 233 - 269 (1997).

86. Carmeliet P & Collen D. Role of Vascular Endothelial Growth Factor and Vascular Endothelial Growth Factor Receptors in Vascular Development. *Curr Top Microbiol Immunol* 237, 133-158 (1999).

87. Ferrara N. Role of Vascular Endothelial Growth Factor in Physiologic and Pathologic Angiogenesis: Therapeutic Implications. *Semin Oncol* 29, 10-14 (2002).

88. Montesano R, Vassalli JD, Baird A, Guillemin R & Orci L. Basic Fibroblast Growth Factor Induces Angiogenesis in Vitro. *Proc Natl Acad Sci U S A* 83, 7297-7301 (1986).

89. Frolik CA, Dart LL, Meyers CA, Smith DM & Sporn MB. Purification and Initial Characterization of a Type Beta Transforming Growth Factor from Human Placenta. *Proc Natl Acad Sci U S A* 80, 3676-3680 (1983).

90. Ross R, Glomset J, Kariya B & Harker L. A Platelet-Dependent Serum Factor That Stimulates the Proliferation of Arterial Smooth Muscle Cells in Vitro. *Proc Natl Acad Sci U S A* 71, 1207-1210 (1974).

91. Leibovich SJ, Polverini PJ, Shepard HM, Wiseman DM, Shively V & Nuseir N. Macrophage-Induced Angiogenesis Is Mediated by Tumour Necrosis Factor-Alpha. *Nature* 329, 630-632 (1987).

92. Fajardo LF, Kwan HH, Kowalski J, Prionas SD & Allison AC. Dual Role of Tumor Necrosis Factor-Alpha in Angiogenesis. *The American journal of pathology* 140, 539-544 (1992).

93. Davis S, Aldrich TH, Jones PF, Acheson A, Compton DL, Jain V, Ryan TE, Bruno J, Radziejewski C, Maisonpierre PC & Yancopoulos GD. Isolation of Angiopoietin-1, a Ligand for the Tie2 Receptor, by Secretion-Trap Expression Cloning. *Cell* 87, 1161-1169 (1996).

94. Valenzuela DM, Griffiths JA, Rojas J, Aldrich TH, Jones PF, Zhou H, McClain J, Copeland NG, Gilbert DJ, Jenkins NA, Huang T, Papadopoulos N, Maisonpierre PC, Davis S & Yancopoulos GD. Angiopoietins 3 and 4: Diverging Gene Counterparts in Mice and Humans. *Proc Natl Acad Sci U S A* 96, 1904-1909 (1999).

95. Maisonpierre PC, Suri C, Jones PF, Bartunkova S, Wiegand SJ, Radziejewski C, Compton D, McClain J, Aldrich TH, Papadopoulos N, Daly TJ, Davis S, Sato TN & Yancopoulos GD. Angiopoietin-2, a Natural Antagonist for Tie2 That Disrupts in Vivo Angiogenesis. *Science* 277, 55-60 (1997).

96. Rosen EM, Zitnik RJ, Elias JA, Bhargava MM, Wines J & Goldberg ID. The Interaction of Hgf-Sf with Other Cytokines in Tumor Invasion and Angiogenesis. *Exs* 65, 301-310 (1993).

97. Sierra-Honigmann MR, Nath AK, Murakami C, Garcia-Cardena G, Papapetropoulos A, Sessa WC, Madge LA, Schechner JS, Schwabb MB, Polverini PJ & Flores-Riveros JR. Biological Action of Leptin as an Angiogenic Factor. *Science* 281, 1683-1686 (1998).

98. West DC, Hampson IN, Arnold F & Kumar S. Angiogenesis Induced by Degradation Products of Hyaluronic Acid. *Science* 228, 1324-1326 (1985).

99. Ribatti D. The Crucial Role of Vascular Permeability Factor/Vascular Endothelial Growth Factor in Angiogenesis: A Historical Review. *Br J Haematol* 128, 303-309 (2005).

100. Dvorak HF, Brown LF, Detmar M & Dvorak AM. Vascular Permeability Factor/Vascular Endothelial Growth Factor, Microvascular Hyperpermeability, and Angiogenesis. *Am J Pathol* 146, 1029-1039 (1995).

101. Senger DR, Galli SJ, Dvorak AM, Perruzzi CA, Harvey VS & Dvorak HF. Tumor Cells Secrete a Vascular Permeability Factor That Promotes Accumulation of Ascites Fluid. *Science* 219, 983-985 (1983).

102. Collins PD, Connolly DT & Williams TJ. Characterization of the Increase in Vascular Permeability Induced by Vascular Permeability Factor in Vivo. *Br J Pharmacol* 109, 195-199 (1993).

103. Dvorak HF, Senger DR, Dvorak AM, Harvey VS & McDonagh J. Regulation of Extravascular Coagulation by Microvascular Permeability. *Science* 227, 1059-1061 (1985).

104. Baumgartner I, Rauh G, Pieczek A, Wuensch D, Magner M, Kearney M, Schainfeld R & Isner JM. Lower-Extremity Edema Associated with Gene Transfer of Naked DNA Encoding Vascular Endothelial Growth Factor. *Ann Intern Med* 132, 880-884 (2000).

105. Baumgartner I, Pieczek A, Manor O, Blair R, Kearney M, Walsh K & Isner JM. Constitutive Expression of Phvegf165 after Intramuscular Gene Transfer Promotes Collateral Vessel Development in Patients with Critical Limb Ischemia. *Circulation* 97, 1114-1123 (1998).

106. Chang LK, Garcia-Cardena G, Farnebo F, Fannon M, Chen EJ, Butterfield C, Moses MA, Mulligan RC, Folkman J & Kaipainen A. Dose-Dependent Response of Fgf-2 for Lymphangiogenesis. *Proc Natl Acad Sci U S A* 101, 11658-11663 (2004).

107. Nagy JA, Vasile E, Feng D, Sundberg C, Brown LF, Detmar MJ, Lawitts JA, Benjamin L, Tan X, Manseau EJ, Dvorak AM & Dvorak HF. Vascular Permeability Factor/Vascular Endothelial Growth Factor Induces Lymphangiogenesis as Well as Angiogenesis. *J Exp Med* 196, 1497-1506 (2002).

108. Meyer K & Palmer JW. The Polysaccharide of the Vitreous Humor. *The Journal of biological chemistry* 107, 629-634 (1934).

109. Jiang D, Liang J & Noble PW. Hyaluronan in Tissue Injury and Repair. *Annual review of cell and developmental biology* 23, 435-461 (2007).

110. Kogan G, Soltes L, Stern R & Gemeiner P. Hyaluronic Acid: A Natural Biopolymer with a Broad Range of Biomedical and Industrial Applications. *Biotechnology letters* 29, 17-25 (2007).

111. Chen WY & Abatangelo G. Functions of Hyaluronan in Wound Repair. *Wound Repair Regen* 7, 79-89 (1999).

112. Allison DD & Grande-Allen KJ. Review. Hyaluronan: A Powerful Tissue Engineering Tool. *Tissue Eng* 12, 2131-2140 (2006).

113. Knudson CB & Knudson W. Hyaluronan-Binding Proteins in Development, Tissue Homeostasis, and Disease. *Faseb J* 7, 1233-1241 (1993).

114. Laurent TC & Fraser JR. Hyaluronan. *Faseb J* 6, 2397-2404 (1992).

115. Toole BP. Hyaluronan in Morphogenesis. *Journal of internal medicine* 242, 35-40 (1997).

116. Zhou B, McGary CT, Weigel JA, Saxena A & Weigel PH. Purification and Molecular Identification of the Human Hyaluronan Receptor for Endocytosis. *Glycobiology* 13, 339-349 (2003).

117. Slevin M, Krupinski J, Gaffney J, Matou S, West D, Delisser H, Savani RC & Kumar S. Hyaluronan-Mediated Angiogenesis in Vascular Disease: Uncovering Rhamm and Cd44 Receptor Signaling Pathways. *Matrix Biol* 26, 58-68 (2007).

118. Balazs EA. Viscoelastic Properties of Hyaluronan and Its Therapeutic Use. in *Chemistry and Biology of Hyaluronan* (eds. Garg HG & Hales CA) 415 (Elsevier, Amsterdam, 2004).

119. Csoka AB, Frost GI & Stern R. The Six Hyaluronidase-Like Genes in the Human and Mouse Genomes. *Matrix Biol* 20, 499-508 (2001).

120. Abatangelo G, Martelli M & Vecchia P. Healing of Hyaluronic Acid-Enriched Wounds: Histological Observations. *J Surg Res* 35, 410-416 (1983).

121. Anderson I. The Properties of Hyaluronan and Its Role in Wound Healing. *Prof Nurse* 17, 232-235 (2001).

122. Bullard KM, Longaker MT & Lorenz HP. Fetal Wound Healing: Current Biology. *World journal of surgery* 27, 54-61 (2003).

123. Laurent C, Hellstrom S & Stenfors LE. Hyaluronic Acid Reduces Connective Tissue Formation in Middle Ears Filled with Absorbable Gelatin Sponge: An Experimental Study. *American journal of otolaryngology* 7, 181-186 (1986).

124. Al Qteishat A, Gaffney JJ, Krupinski J & Slevin M. Hyaluronan Expression Following Middle Cerebral Artery Occlusion in the Rat. *Neuroreport* 17, 1111-1114 (2006).

125. Funakoshi T, Majima T, Iwasaki N, Suenaga N, Sawaguchi N, Shimode K, Minami A, Harada K & Nishimura S. Application of Tissue Engineering Techniques for Rotator Cuff Regeneration Using a Chitosan-Based Hyaluronan Hybrid Fiber Scaffold. *Am J Sports Med* 33, 1193-1201 (2005).

126. Rooney P, Kumar S, Ponting J & Wang M. The Role of Hyaluronan in Tumour Neovascularization (Review). *Int J Cancer* 60, 632-636 (1995).

127. Stern R, Asari AA & Sugahara KN. Hyaluronan Fragments: An Information-Rich System. *European journal of cell biology* 85, 699-715 (2006).

128. Arnold F, West DC, Schofield PF & Kumar S. Angiogenic Activity in Human Wound Fluid. *Int J Microcirc Clin Exp* 5, 381-386 (1987).

129. Lees VC, Fan TP & West DC. Angiogenesis in a Delayed Revascularization Model Is Accelerated by Angiogenic Oligosaccharides of Hyaluronan. *Lab Invest* 73, 259-266 (1995).

130. Slevin M, Kumar S & Gaffney J. Angiogenic Oligosaccharides of Hyaluronan Induce Multiple Signaling Pathways Affecting Vascular

Endothelial Cell Mitogenic and Wound Healing Responses. *J Biol Chem* 277, 41046-41059 (2002).

131. Noble PW, McKee CM, Cowman M & Shin HS. Hyaluronan Fragments Activate an Nf-Kappa B/I-Kappa B Alpha Autoregulatory Loop in Murine Macrophages. *J Exp Med* 183, 2373-2378 (1996).

132. McKee CM, Penno MB, Cowman M, Burdick MD, Strieter RM, Bao C & Noble PW. Hyaluronan (Ha) Fragments Induce Chemokine Gene Expression in Alveolar Macrophages. The Role of Ha Size and Cd44. *J Clin Invest* 98, 2403-2413 (1996).

133. Zeng C, Toole BP, Kinney SD, Kuo JW & Stamenkovic I. Inhibition of Tumor Growth in Vivo by Hyaluronan Oligomers. *Int J Cancer* 77, 396-401 (1998).

134. Ghatak S, Misra S & Toole BP. Hyaluronan Oligosaccharides Inhibit Anchorage-Independent Growth of Tumor Cells by Suppressing the Phosphoinositide 3-Kinase/Akt Cell Survival Pathway. *J Biol Chem* 277, 38013-38020 (2002).

135. Aruffo A, Stamenkovic I, Melnick M, Underhill CB & Seed B. Cd44 Is the Principal Cell Surface Receptor for Hyaluronate. *Cell* 61, 1303-1313 (1990).

136. Underhill C. Cd44: The Hyaluronan Receptor. *Journal of cell science* 103 (Pt 2), 293-298 (1992).

137. Lesley J, Hyman R & Kincade PW. Cd44 and Its Interaction with Extracellular Matrix. *Advances in immunology* 54, 271-335 (1993).

138. Culty M, Nguyen HA & Underhill CB. The Hyaluronan Receptor (Cd44) Participates in the Uptake and Degradation of Hyaluronan. *The Journal of cell biology* 116, 1055-1062 (1992).

139. Hua Q, Knudson CB & Knudson W. Internalization of Hyaluronan by Chondrocytes Occurs Via Receptor-Mediated Endocytosis. *Journal of cell science* 106 (Pt 1), 365-375 (1993).

140. Turley EA. Hyaluronan and Cell Locomotion. *Cancer metastasis reviews* 11, 21-30 (1992).

141. Was H. [Characterization of Markers and Growth Factors for Lymphatic Endothelium]. *Postepy biochemii* 51, 209-214 (2005).

142. Banerji S, Ni J, Wang SX, Clasper S, Su J, Tammi R, Jones M & Jackson DG. Lyve-1, a New Homologue of the Cd44 Glycoprotein, Is a Lymph-Specific Receptor for Hyaluronan. *The Journal of cell biology* 144, 789-801 (1999).

143. Ades EW, Candal FJ, Swerlick RA, George VG, Summers S, Bosse DC & Lawley TJ. Hmec-1: Establishment of an Immortalized Human Microvascular Endothelial Cell Line. *The Journal of investigative dermatology* 99, 683-690 (1992).

144. Sarasam A & Madihally SV. Characterization of Chitosan-Polycaprolactone Blends for Tissue Engineering Applications. *Biomaterials* 26, 5500-5508 (2005).

145. Mondalek FG, Zhang YY, Kropp B, Kopke RD, Ge X, Jackson RL & Dormer KJ. The Permeability of Spion over an Artificial Three-Layer Membrane Is Enhanced by External Magnetic Field. *J Nanobiotechnology* 4, 4 (2006).

146. Selvakumaran M, Lin HK, Sjin RT, Reed JC, Liebermann DA & Hoffman B. The Novel Primary Response Gene Myd118 and the Proto-Oncogenes Myb, Myc, and Bcl-2 Modulate Transforming Growth Factor Beta 1-Induced Apoptosis of Myeloid Leukemia Cells. *Molecular and cellular biology* 14, 2352-2360 (1994).

147. Kropp BP, Cheng EY, Pope JCt, Brock JW, 3rd, Koyle MA, Furness PD, 3rd, Weigel ND, Keck RW & Kropp KA. Use of Small Intestinal Submucosa for Corporal Body Grafting in Cases of Severe Penile Curvature. *J Urol* 168, 1742-1745; discussion 1745 (2002).

148. Colvert JR, 3rd, Kropp BP, Cheng EY, Pope JCt, Brock JW, 3rd, Adams MC, Austin P, Furness PD, 3rd & Koyle MA. The Use of Small Intestinal Submucosa as an Off-the-Shelf Urethral Sling Material for Pediatric Urinary Incontinence. *J Urol* 168, 1872-1875; discussion 1875-1876 (2002).

149. Bhang SH, Lim JS, Choi CY, Kwon YK & Kim BS. The Behavior of Neural Stem Cells on Biodegradable Synthetic Polymers. *Journal of biomaterials science* 18, 223-239 (2007).

150. Pattison M, Webster TJ, Leslie J, Kaefer M & Haberstroh KM. Evaluating the in Vitro and in Vivo Efficacy of Nano-Structured Polymers for Bladder Tissue Replacement Applications. *Macromolecular bioscience* 7, 690-700 (2007).

151. Nuininga JE, van Moerkerk H, Hanssen A, Hulsbergen CA, Oosterwijk-Wakka J, Oosterwijk E, de Gier RP, Schalken JA, van Kuppevelt TH & Feitz WF. A Rabbit Model to Tissue Engineer the Bladder. *Biomaterials* 25, 1657-1661 (2004).

152. Cartwright LM, Shou Z, Yeger H & Farhat WA. Porcine Bladder Acellular Matrix Porosity: Impact of Hyaluronic Acid and Lyophilization. *J Biomed Mater Res A* 77, 180-184 (2006).

153. Brown AL, Ringuette MJ, Prestwich GD, Bagli DJ & Woodhouse KA. Effects of Hyaluronan and Sparc on Fibroproliferative Events Assessed in an in Vitro Bladder Acellular Matrix Model. *Biomaterials* 27, 3825-3835 (2006).

154. Roth CC, Bell CH, Woodson B, Schultz AD, Palmer BW, Frimberger D, Fung KM, Lin HK & Kropp BP. Temporal Differentiation and Maturation of Regenerated Rat Urothelium. *BJU Int* 103, 836-841 (2009).

155. Ashley RA, Palmer BW, Schultz AD, Woodson BW, Roth CC, Routh JC, Fung KM, Frimberger D, Lin HK & Kropp B. Leukocyte Inflammatory

Response in a Rat Urinary Bladder Regeneration Model Using Porcine Small Intestinal Submucosa Scaffold. *Tissue Eng Part A*, in press (2009).

156. Fung KM, Samara EN, Wong C, Metwalli A, Krlin R, Bane B, Liu CZ, Yang JT, Pitha JV, Culkin DJ, Kropp BP, Penning TM & Lin HK. Increased Expression of Type 2 3α-Hydroxysteroid Dehydrogenase/Type 5 17β-Hydroxysteroid Dehydrogenase (Akr1c3) and Its Relationship with Androgen Receptor in Prostate Carcinoma. *Endocrine-related cancer* 13, 169-180 (2006).

157. Mast BA, Flood LC, Haynes JH, DePalma RL, Cohen IK, Diegelmann RF & Krummel TM. Hyaluronic Acid Is a Major Component of the Matrix of Fetal Rabbit Skin and Wounds: Implications for Healing by Regeneration. *Matrix (Stuttgart, Germany)* 11, 63-68 (1991).

158. Pothacharoen P, Siriaunkgul S, Ong-Chai S, Supabandhu J, Kumja P, Wanaphirak C, Sugahara K, Hardingham T & Kongtawelert P. Raised Serum Chondroitin Sulfate Epitope Level in Ovarian Epithelial Cancer. *Journal of biochemistry* 140, 517-524 (2006).

159. Dechert TA, Ducale AE, Ward SI & Yager DR. Hyaluronan in Human Acute and Chronic Dermal Wounds. *Wound Repair Regen* 14, 252-258 (2006).

160. Cao G, Savani RC, Fehrenbach M, Lyons C, Zhang L, Coukos G & Delisser HM. Involvement of Endothelial Cd44 During in Vivo Angiogenesis. *The American journal of pathology* 169, 325-336 (2006).

161. Witt M & Kasper M. Immunohistochemical Distribution of Cd44 and Some of Its Isoforms During Human Taste Bud Development. *Histochemistry and cell biology* 110, 95-103 (1998).

162. Yamazaki M, Nakajima F, Ogasawara A, Moriya H, Majeska RJ & Einhorn TA. Spatial and Temporal Distribution of Cd44 and Osteopontin in Fracture Callus. *The Journal of bone and joint surgery* 81, 508-515 (1999).

163. Knudson CB. Hyaluronan and Cd44: Strategic Players for Cell-Matrix Interactions During Chondrogenesis and Matrix Assembly. *Birth Defects Res C Embryo Today* 69, 174-196 (2003).

164. Johnson LA, Prevo R, Clasper S & Jackson DG. Inflammation-Induced Uptake and Degradation of the Lymphatic Endothelial Hyaluronan Receptor Lyve-1. *The Journal of biological chemistry* 282, 33671-33680 (2007).

165. Toole BP, Munaim SI, Welles S & Knudson CB. Hyaluronate-Cell Interactions and Growth Factor Regulation of Hyaluronate Synthesis During Limb Development. *Ciba Foundation symposium* 143, 138-145 (1989).

166. Mast BA, Frantz FW, Diegelmann RF, Krummel TM & Cohen IK. Hyaluronic Acid Degradation Products Induce Neovascularization and Fibroplasia in Fetal Rabbit Wounds. *Wound Repair Regen* 3, 66-72 (1995).

167. Nesti LJ, Li WJ, Shanti RM, Jiang YJ, Jackson W, Freedman BA, Kuklo TR, Giuliani JR & Tuan RS. Intervertebral Disc Tissue Engineering Using a

Novel Hyaluronic Acid-Nanofibrous Scaffold (Hanfs) Amalgam. *Tissue engineering* 14, 1527-1537 (2008).

168. Hoeppner J, Crnogorac V, Marjanovic G, Juttner E, Karcz W, Weiser HF & Hopt UT. Small Intestinal Submucosa as a Bioscaffold for Tissue Regeneration in Defects of the Colonic Wall. *J Gastrointest Surg* 13, 113-119 (2009).

169. Astete CE & Sabliov CM. Synthesis and Characterization of Plga Nanoparticles. *J Biomater Sci Polym Ed* 17, 247-289 (2006).

170. Mondalek FG, Lawrence BJ, Kropp BP, Grady BP, Fung KM, Madihally SV & Lin HK. The Incorporation of Poly(Lactic-Co-Glycolic) Acid Nanoparticles into Porcine Small Intestinal Submucosa Biomaterials. *Biomaterials* 29, 1159-1166 (2008).

171. Storgard C, Mikolon D & Stupack DG. Angiogenesis Assays in the Chick Cam. *Methods Mol Biol* 294, 123-136 (2005).

172. Gao F, Cao M, Yang C, He Y & Liu Y. Preparation and Characterization of Hyaluronan Oligosaccharides for Angiogenesis Study. *Journal of biomedical materials research* 78, 385-392 (2006).

173. Hans ML & Lowman AM. Biodegradable Nanoparticles for Drug Delivery and Targeting. *Curr Opin Solid State Mater Sci* 6, 319-327 (2002).

174. Alkrad JA, Mrestani Y, Stroehl D, Wartewig S & Neubert R. Characterization of Enzymatically Digested Hyaluronic Acid Using Nmr, Raman, Ir, and Uv-Vis Spectroscopies. *Journal of pharmaceutical and biomedical analysis* 31, 545-550 (2003).

175. Trimm HH & Jennings BR. Study of Hyaluronic Acid Flexibility by Electric Birefringence. *The Biochemical journal* 213, 671-677 (1983).

176. Mitra AK, Arnott S & Sheehan JK. Hyaluronic Acid: Molecular Conformation and Interactions in the Tetragonal Form of the Potassium Salt Containing Extended Chains. *Journal of molecular biology* 169, 813-827 (1983).

177. Hamann KJ, Dowling TL, Neeley SP, Grant JA & Leff AR. Hyaluronic Acid Enhances Cell Proliferation During Eosinopoiesis through the Cd44 Surface Antigen. *J Immunol* 154, 4073-4080 (1995).

178. Morra M. Engineering of Biomaterials Surfaces by Hyaluronan. *Biomacromolecules* 6, 1205-1223 (2005).

179. Mast BA, Diegelmann RF, Krummel TM & Cohen IK. Hyaluronic Acid Modulates Proliferation, Collagen and Protein Synthesis of Cultured Fetal Fibroblasts. *Matrix (Stuttgart, Germany)* 13, 441-446 (1993).

180. Cabrera RC, Siebert JW, Eidelman Y, Gold LI, Longaker MT & Garg HG. The in Vivo Effect of Hyaluronan Associated Protein-Collagen Complex on Wound Repair. *Biochemistry and molecular biology international* 37, 151-158 (1995).

181. Olutoye OO, Barone EJ, Yager DR, Uchida T, Cohen IK & Diegelmann RF. Hyaluronic Acid Inhibits Fetal Platelet Function: Implications in Scarless Healing. *Journal of pediatric surgery* 32, 1037-1040 (1997).

Abbreviations

AF: Angiogenic factors

CD44: Cluster of differentiation 44

DAB: 3,3'-Diaminobenzidine

ddH_2O: Double distilled water

DLS: Dynamic light scattering

ECM: Extracellular matrix

FBS: Fetal bovine serum

FGF: Fibroblast growth factor

GAG: Glycosaminoglycan

HA: Hyaluronic acid

HA-PLGA-SIS: SIS modified with HA-PLGA NPs

HARE: Hyaluronic acid receptor for endocytosis

HMEC-1: Human microvascular endothelial cells

HRP: Horseradish peroxidase

LYVE-1: Lymph vessel endothelial receptor 1

MW: Molecular weight

NPs: nanoparticles

PBS: Phosphate buffer saline

PDGF: Platelet derived growth factor

PEI: poly(ethyleneimine)

PGA: Poly(glycolic acid)

PLA: Poly(lactic acid)

PLGA: Poly(lactide-co-glycolide) acid also known as poly(lactic-co-glycolic) acid

PVA: Poly(vinyl alcohol)

RHAMM: Receptor for hyaluronic acid mediated motility

SEM: Scanning electron microscope

SIS: small intestinal submucosa

TGF: Transforming growth factor

TNE: Tris-HCl + NaCl + EDTA

TNF: Tumor necrosis factor

VEGF: Vascular endothelial growth factor

VEGFR-3: Vascular endothelial growth factor receptor 3

VPF: Vascular permeability factor